Tianjin Daxue Xuebao (Ziran Kexue yu Gongcheng Jishu Ban)/
Journal of Tianjin University Science and Technology
ISSN (Online):0493-2137
E-Publication: Online Open Access
Vol: 55 Issue: 10:2022
DOI: 10.5281/zenodo.19248091

EXPERIMENTAL INVESTIGATION OF LUBRICANT STARVATION ON THE TRIBO PERFORMANCE OF EHD LINE CONTACT

Dr. SURESH JADHAV*
Assistant Professor, Department of Mechanical Engineering VJTI Matunga, Mumbai, India. *Corresponding Author Email: sgjadhav@me.vjti.ac.in

GANANATH D. THAKRE
Advanced Tribology Research Centre, CSIR-IIP Dehradun, India.

Abstract

Non-conformal EHL line contact frequently operate under server starved lubrication. This is commonly correlated to EHL regimes resulting in reduced lifespan. Consequently, the purpose of this work is to explore the influence of starved lubricant regime on the tribo-performances behaviour of EHD line contact. In the present study, numerical simulation and experimental investigation emphasizes the importance of using lubricant properties response of commercial oils for accurate prediction of EHL characteristics in line contact. Lubricated worn out test specimen surface structures were investigated by measuring the wear and contact friction behaviour in the block-on-roller tribo test rig. Experimental result reveals that wear or failure and contact friction of the surface has been increased under starvation lubricant regime. Surface topography has been constructed sufficiently according to the operating condition of the tribo-pair contact. Microscope and 3D profilometry analysis showed that worn out test specimen surface could show higher wear and contact friction. Numerical simulated results presented, as the position of inlet meniscus moves closer to Hertizian contact an increase in percentage of starvation is observed with increase in speed. Which results, pressure spike and fluid film profile reduction in the contact.

Keywords: Starved Lubrication, Elastohydrodynamic Lubrication (EHL), Friction, Wear, Micro Structure Analysis, Surface Topography.

1. INTRODUCTION

Mechanical components operating in EHL may be subjected to extremely high and dynamic loads, fluctuating operating parameters, elevated temperatures, deterioration of lubricant properties due to contamination or chemical reactions, surface wear etc. These conditions may result in catastrophic failure of machines in the absence of stringent design measures. Non-conformal contacts are found in many machine elements such as rolling bearings, cams and follower, linear reciprocating bearings, gear sets etc. The concentrated contacts in these machine elements experience high contact pressures normally varying in the range of 0.5 - 4 GPa and are often subjected to operate in the mixed/boundary lubrication regimes, which are undesirable situations from the tribological point of view. Moreover, it is worth mentioning here that generally non- conformal contacts possess less tribological performance due to the lack of existence of thick lubricating film at the interface. Therefore, the fluid film is not capable to maintain full separation of moving surfaces, which leads to excessive heat and friction, wear, noise, vibration and subsequently seizure of moving sliding/rolling elements. This is not a favorable condition for suppressing the wear and contact friction of rolling/sliding concentrated contacts in precision machinery. A partial absence of oil in the machine element typically leads to

Tianjin Daxue Xuebao (Ziran Kexue yu Gongcheng Jishu Ban)/
Journal of Tianjin University Science and Technology
ISSN (Online):0493-2137
E-Publication: Online Open Access
Vol: 55 Issue: 10:2022
DOI: 10.5281/zenodo.19248091

seizure of the mechanical system and total failure of the engine. This kind of failure is termed as premature failure and concern with a catastrophic or functional event. Catastrophic failures can cause damage not just to the specific component in question but also collateral damage. In other words, causes significant collateral damage, production interruption and/or the occurrence of a safety hazard. But tribologist state a frequent issue with respect to lacking oiling. The absence of a proper oil film will result in metal-to-metal contact. Effect of oil starvation of machine element is presented in the Figure 1.EHL contact zone is comprised of an inlet (low-pressure) zone, outlet (cavitation) zone and central (high-pressure) zone. The central (high-pressure) zone is fully flooded and outlet and inlet region are partially flooded. The X_{in} is the inlet meniscus is the point where the fluid film height of the surfaces flow together due to elastic deformation and geometry of the EHL contact. Starved lubrication condition exists if low pressure (inlet) region is partially flooded and fluid film thickness in the high-pressure (central contact) zone has less compared to the fully flooded inlet region. Pressure spike diminishes in the outlet zone due to the inlet distance shifting towards the contact zone[1-3].

Lubricated concentrated contacts are found to be beneficial in minimizing the surface damage during the start-up and reversal of motions[4, 5]. Under parched lubricated conditions, fluid film thickness can be much thinner than that of fully flooded conditions have been reported by Hamrock-Dowson prediction[2]. This conditions can cause reduction in the fluid film thickness and thus the contact pressure increase as well as excessive wear and friction caused by direct surface interactions. Wedeven et al.[6]experimentally demonstrated that the effect of the starvation on film thickness in EHL contacts. In this work, influence of the starvation on the behavior of fluid film in EHL contact have been described using optical interferometry technique. Chiu[7] and Pemberton and Cameron[8]have been carried out experimental works, find out the relationship between lubricant supply conditions in the inlet region and fluid film thickness. And also presented the effect of oil-air meniscus formation at the inlet on fluid film thickness in the contact area. Oil Starvation and cross flow in a starved non-conformal contact have been examined by Kingsbury [9, 10]. For starved contacts, fluid film thickness relation founded by Wolveridge et al.[11]. This approach based upon reduction in fluid film thickness and position of inlet meniscus in line contacts [2]. They presented numerically the relation between fluid film thickness and upstream boundary in EHL point contact. This is not suitable in the engineering application, because in the actual practice inlet meniscus position cannot be determine. Elrod[12]developed suitable numerical algorithm to handle boundary between cavitated and starved zones. In this approach input parameter has been considered thickness of oil layer on a surface. Recently, Venner et al. [13], Wijnant [14] Chevalier et al.[13] and Damiens et al.[15] have been made enormous effort to describe the role of Elrod algorithm in the mechanism of starved EHL point contacts. The simplified method for the film thickness calculation was presented by[13, 15] based on results obtained from starved EHL contact. Therefore, theoretical model is appropriate for elliptical and circular conjunctions. Bioboulet et al. [16] analyzed the load carrying capacity, the Poiseuille and Couette flow based on friction, as a function of the degree of starvation. It was shown that the Poiseuille friction force diminishes fastest with starvation,

Tianjin Daxue Xuebao (Ziran Kexue yu Gongcheng Jishu Ban)/
Journal of Tianjin University Science and Technology
ISSN (Online):0493-2137
E-Publication: Online Open Access
Vol: 55 Issue: 10:2022
DOI: 10.5281/zenodo.19248091

load carrying capacity and finally the Couette term diminishes slowest of all three terms. Muller et al.[17] presented a detailed modeling of fluid flow through a tribological interface under starved lubrication conditions. In spite of the significance of the starvation in the EHL, scanty numbers of studies have been available related to the starvation in the EHL. In the present work, the numerical and experimental methodology carried out in non-conformal EHL line contact, to take lubricant starvation into consideration.

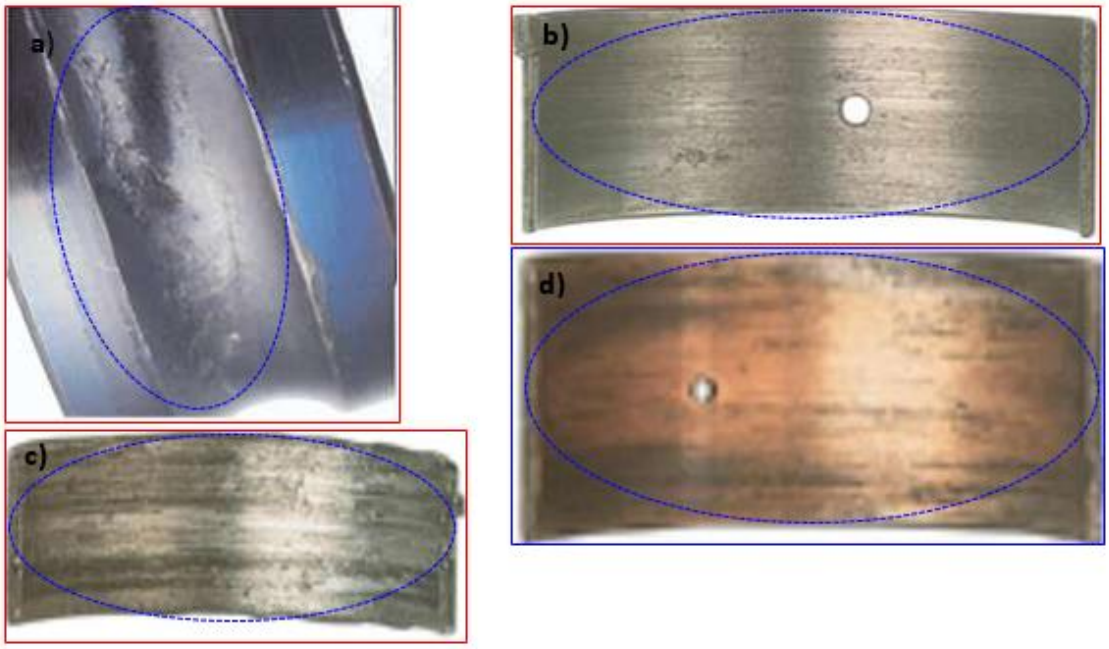

Figure 1: Effect of oil starvation or oil supply on machine element [25,26]

2. BACKGROUND

In the present study, all experimental investigations carried out on the block-on-roller tribo test rig. The tribo-test rig not only evaluates the tribological behavior of lubricants, it also helps understand the correlation between tribological properties and rheological properties of servo gear oil HP140 (28-34 cSt @ 100°C) and SAE 75W80 (13.5-15.5 cSt @ 100°C) due to their direct mutual influence on each other.

Lubricants used in this experiments are servo gear oil HP140 and SAE 75W80.Surface roughness Ra = 0.6 to 0.8mm and 65 HRC has been used for the experimentations. In the present study, when inlet contact does not fill sufficiently with lubricant then there is shortage of lubricant in the contact area, which leads to thin film and even breakdown takes place. It is known as starvation effect, the effect of starvation is observed at different values of loads and velocities. In this study, a systematic approach of numerical simulation and experimental testing were planned.

Tianjin Daxue Xuebao (Ziran Kexue yu Gongcheng Jishu Ban)/
Journal of Tianjin University Science and Technology
ISSN (Online):0493-2137
E-Publication: Online Open Access
Vol: 55 Issue: 10:2022
DOI: 10.5281/zenodo.19248091

3. ANALYTICAL FORMULATION

3.1 Governing equations

The analysis of non-conformal EHL line contacts for a Servo Gear HP 140 and Gear oil 75W80 lubricant involves the coupled solution of Reynolds equation, fluid film thickness equation and force equilibrium equation subjected to the appropriate boundary conditions with due consideration to the rheology and variation of the rheological properties. Reynolds equation for 1D EHL contact can be expressed as[18]:

$$\frac{\partial}{\partial x}\left[\frac{\rho h^3}{12\eta}\frac{\partial p}{\partial x}\right]=u_s\left[\frac{\partial(\rho h)}{\partial x}\right] \tag{1}$$

here $u_s=\frac{u_1+u_2}{2}$

Following dimensionless parameters are used:

$$X=X/a;P=p/p_h;H=hR/a^2;\bar{\rho}=\rho/\rho_0;\bar{\eta}=\eta/\eta_0$$

Equation (1) is expressed in non-dimensional form using dimensionless parameters

$$\frac{\partial}{\partial X}\left[\frac{\bar{\rho}H^3}{12\bar{\eta}}\frac{\partial P}{\partial X}\right]=\Omega\left[\frac{\partial(\bar{\rho}H)}{\partial X}\right] \tag{2}$$

where $\Omega=3U\pi^2/4W^2$

To solve the Reynolds equation, following boundary condition are applied[18]:

$$\mathrm{P}=0 \text{ at } \mathrm{X}=\mathrm{X}_{\mathrm{in}} \;;\; \mathrm{P}=\frac{\mathrm{dP}}{\mathrm{dX}} \text{ at } \mathrm{X}=\mathrm{X}_{\mathrm{o}}$$

Here, X_{in} = Inlet boundary condition and X_o = Outlet boundary condition.

Elasticity equation includes the undeformed term and elastic deformation term for a given pressure distribution[18]. In this study, lubricant film thickness can be written as:

$$\mathrm{H}=\mathrm{H}_0+\frac{\mathrm{X}^2}{2}-\frac{1}{\pi}\int_{-\infty}^{\infty}\ln\left|\mathrm{X}-\mathrm{X}'\right|\mathrm{P}(\mathrm{X}')\mathrm{dX}' \tag{3}$$

Dimensionless form of density-pressure relation [18] is expressed as:

$$\bar{\rho}=\left(1+\frac{0.6\times10^{-6}\mathrm{P}.\mathrm{P}_{\mathrm{h}}}{1+1.7\times10^{-9}\mathrm{P}.\mathrm{P}_{\mathrm{h}}}\right) \tag{4}$$

Tianjin Daxue Xuebao (Ziran Kexue yu Gongcheng Jishu Ban)/
Journal of Tianjin University Science and Technology
ISSN (Online):0493-2137
E-Publication: Online Open Access
Vol: 55 Issue: 10:2022
DOI: 10.5281/zenodo.19248091

Dimensionless form of Viscosity-pressure relation[19] is given by

$$\bar{\eta} = \exp\left\{ (\ln\eta_0 + 9.67)\left\{-1+\left(1+5.1\times10^{-9}\,\mathrm{P}.\mathrm{P}_h\right)^z\right\}\right\} \tag{5}$$

The applied load is supported by the pressure developed within the lubricant film, therefore to satisfy the force balance condition, pressure obtained from the Reynolds equation should be equal to external load[18].Equation can be written in dimensionless form as:

$$\int_{x_i}^{x_o} P dX = \pi / 2 \tag{6}$$

The governing equations are solved to obtain pressure distribution and film shape which is used to evaluate the coefficient of friction[18] which is expressed iAn dimensionless form is:

$$\mu = -\sqrt{\frac{8W}{\pi^3}}\int_{x_{in}}^{x_o} H\left(\frac{dP}{dX}\right)dX \tag{7}$$

3.2 Numerical Procedure

Reynolds equation in EHL line contact modelling problem is convection dominated, using FEM formulation scheme and solved along with the load equilibrium condition using Newton-Raphson method. FEM analysis is able to provide stable solution for the problem. In the present work, the finite element discontinuous Galerkin's method has been used to formulate the EHL line contact modelling problem considering a block-on-roller contact geometry. The Lagrangian shape function is used for interpolating fluid film pressure over the element. The residue of equation (2) is expressed as:

$$\mathrm{R}^e = \frac{\partial}{\partial\bar{\mathrm{x}}}\left[\frac{\bar{\rho}\bar{\mathrm{h}}^3}{\bar{\eta}}\frac{\partial\bar{\mathrm{p}}}{\partial\bar{\mathrm{x}}}\right] - \Omega\frac{\partial\left(\bar{\rho}\bar{\mathrm{h}}\right)}{\partial\bar{\mathrm{x}}} \tag{8}$$

Using orthogonality conditions, Galerkin's method is employed to obtain the following integral equation.

$$\int_{\Omega^e} \mathrm{W}\mathrm{R}_i^e \mathrm{dx} = 0 \tag{9}$$

$$\int_{\Omega^e} \mathrm{W}\frac{\partial}{\partial\bar{\mathrm{x}}}\left[\frac{\bar{\rho}\bar{\mathrm{h}}^3}{\bar{\eta}}\frac{\partial\bar{\mathrm{p}}}{\partial\bar{\mathrm{x}}}\right]\mathrm{dx} - \mathrm{W}\Omega\frac{\partial\left(\bar{\rho}\,\bar{\mathrm{h}}\right)}{\partial\bar{\mathrm{x}}}\mathrm{dx} = 0 \tag{10}$$

Differentiation of any two functions $(\mathrm{f}_1, \mathrm{f}_2)$ is

$$\frac{\mathrm{d}\left(\mathrm{f}_1\mathrm{f}_2\right)}{\mathrm{dx}} = \mathrm{f}_1\frac{\mathrm{df}_2}{\mathrm{dx}} + \mathrm{f}_2\frac{\mathrm{df}_1}{\mathrm{dx}} \tag{11}$$

Tianjin Daxue Xuebao (Ziran Kexue yu Gongcheng Jishu Ban)/
Journal of Tianjin University Science and Technology
ISSN (Online):0493-2137
E-Publication: Online Open Access
Vol: 55 Issue: 10:2022
DOI: 10.5281/zenodo.19248091

Using equation (11), equation (10) is transformed to,

$$\sum_{\Gamma}\left(\frac{W\bar{\rho}\,\bar{h}^3}{\bar{\eta}}\xi_M\frac{\partial\bar{p}}{\partial\bar{x}}\right)-\int_{\Omega^e}\frac{\rho\bar{h}^3}{\bar{\eta}}\xi_M\frac{\partial\bar{p}}{\partial\bar{x}}\frac{\partial W}{\partial\bar{x}}d\bar{x}-\Omega\sum_{\Gamma}\left(W\bar{\rho}\,\bar{h}\right)+\Omega\int_{\Omega^e}\frac{\bar{\rho}\,\bar{h}\partial(W)}{\partial\bar{x}}d\bar{x}=0 \qquad (12)$$

In this method, weighted function W is interchanged by the shape function of pressure i.e. primary variable. The solution is therefore expressed as:

$$\bar{p}=\sum_{i=1}^{p^{e+1}}N_i\bar{p}_i$$

$$N_1(\xi)=\frac{1-\xi}{2}\ \text{ and }\ N_2(\xi)=\frac{1+\xi}{2} \qquad (13)$$

$$\sum_{j=1}^{2}\left[\int_{\Omega^e}\left[\frac{\bar{\rho}\bar{h}^3}{12\bar{\eta}}\xi_M\frac{\partial N_i}{\partial\bar{x}}\frac{\partial N_j}{\partial\bar{x}}dx\right]\bar{p}_j\right]=\frac{\Omega}{2}\int_{\Omega^e}\left(\bar{\rho}\,\bar{h}\right)\frac{\partial N_i}{\partial\bar{x}}dx$$
$$+\sum_{\Gamma}\frac{W\bar{\rho}\bar{h}^3}{12\bar{\eta}}\xi_M\frac{\partial N_j}{\partial\bar{x}}\bar{p}_j \qquad (14)$$
$$-\frac{\Omega}{2}\sum_{\Gamma}\left(N_i\bar{\rho}\,\bar{h}\right)$$

The elemental system of equation is obtained by simplifying equation (14) by using part-wise integration which is stated below as:

$$\left[F_{ij}^e\right]\left\{\bar{p}_j^{\,e}\right\}=\Omega\left\{R_i^e\right\}$$

where

$$\left[F_{ij}^e\right]=\int_{\Omega^e}\left[\frac{\bar{\rho}\bar{h}^3}{12\bar{\eta}}\frac{\partial N_i}{\partial\bar{x}}\frac{\partial N_j}{\partial\bar{x}}dx\right]$$

$$\left\{R_i^e\right\}=\int_{\Omega^e}\left(\bar{\rho}\,\bar{h}\right)\frac{\partial N_i}{\partial\bar{x}}dx$$

Elasticity equation considering a new kernel [20] has been evaluated for elastic deformation as:

$$H(X)=H_0+\frac{X^2}{2}-\frac{1}{\pi}\sum_{e=1}^{N}\int\ln\left|X-X'\right|\sum_{i=1}^{p^e+1}N_i\bar{p}_i(X')dX' \qquad (15)$$

$$H(X)=H_0+\frac{X^2}{2}-\frac{1}{\pi}\sum_{e=1}^{N}\sum_{i=1}^{p^e+1}K_i^e(X)\bar{p}_i^e \qquad (16)$$

Tianjin Daxue Xuebao (Ziran Kexue yu Gongcheng Jishu Ban)/
Journal of Tianjin University Science and Technology
ISSN (Online):0493-2137
E-Publication: Online Open Access
Vol: 55 Issue: 10:2022
DOI: 10.5281/zenodo.19248091

where $K_i^e(X)$ represents the kernel can be expressed as:

$$K_i^e(X) = \int \ln\left|X - X'\right| N_i^e(X')\,dX'$$

$$K_i^e(X) = \frac{h^e}{2}\sum_{i=1}^{m}\left(\ln\left|X - X'(\xi_i)\right| N_i^e(\xi_i)\right) w_i$$

Load balance equation is discretized as [21]:

$$\sum_{e=1}^{N}\sum_{i=1}^{p^e+1} p_i^e N_i^e(X)\,dX - \frac{\pi}{2} = 0 \tag{17}$$

Using Gaussian quadrature, load equilibrium equation can be given as:

$$\sum_{e=1}^{N}\sum_{i=1}^{p^e+1} p_i^e N_i^e \left|J\right| w - \frac{\pi}{2} = 0$$

Coefficient of friction is discretized as:

$$\mu = -\sqrt{\frac{8W}{\pi^3}}\sum_{e=1}^{N}\sum_{i=1}^{p^e+1} H P_i^{e+1}\frac{dN_i^e(X)}{dX}\,dX = 0 \tag{18}$$

Using Gaussian quadrature, Coefficient of friction is expressed as:

$$\mu = -\sqrt{\frac{8W}{\pi^3}}\sum_{e=1}^{N}\sum_{i=1}^{p^e+1} H P_i^e \frac{dN_i^e}{dX}\left|J\right| W$$

4. EXPERIMENTAL STUDY

4.1 Experimental setup and parameters

The lubricant to be tested is introduced in the stationary oil reservoir pot forming thin lubricating film between the block-on-roller and contact geometry are presented in figure 2. The test specimen(block) is made up of AISI chrome alloy standard steel No. E-52100.The block is fixed into the test specimen holder and roller is free to rotate about their own axis. block-on-roller tests were performed as per ASTM D: 4172 standard test procedure. The block-on-roller tribo test rig is generally employed to compute tribo-performance behaviour of non-conformal contacts of machine elements e.g. rolling bearings, cam and gears. Roller is partly submerged in the oil reservoir and loaded against a flat moving surface. Lubricant starvation in the contact has been created by gradually reducing supply amount of oil in the pot. Therefore, restricted amount of lubricant is used in the starvation experimentation. The contact friction in terms of

Tianjin Daxue Xuebao (Ziran Kexue yu Gongcheng Jishu Ban)/
Journal of Tianjin University Science and Technology
ISSN (Online):0493-2137
E-Publication: Online Open Access
Vol: 55 Issue: 10:2022
DOI: 10.5281/zenodo.19248091

frictional torque is continuously recorded during the entire test duration. Each of the oil samples is tested twice and the wear track along the horizontal axis is measured for all the block specimen surfaces thus providing 12 readings for each given oil. The average of the 24 test run is reported as the wear track. At the end of the test, with the aid of microscope wear track has been measured on the test specimen and which is find out contact wear between block and roller.

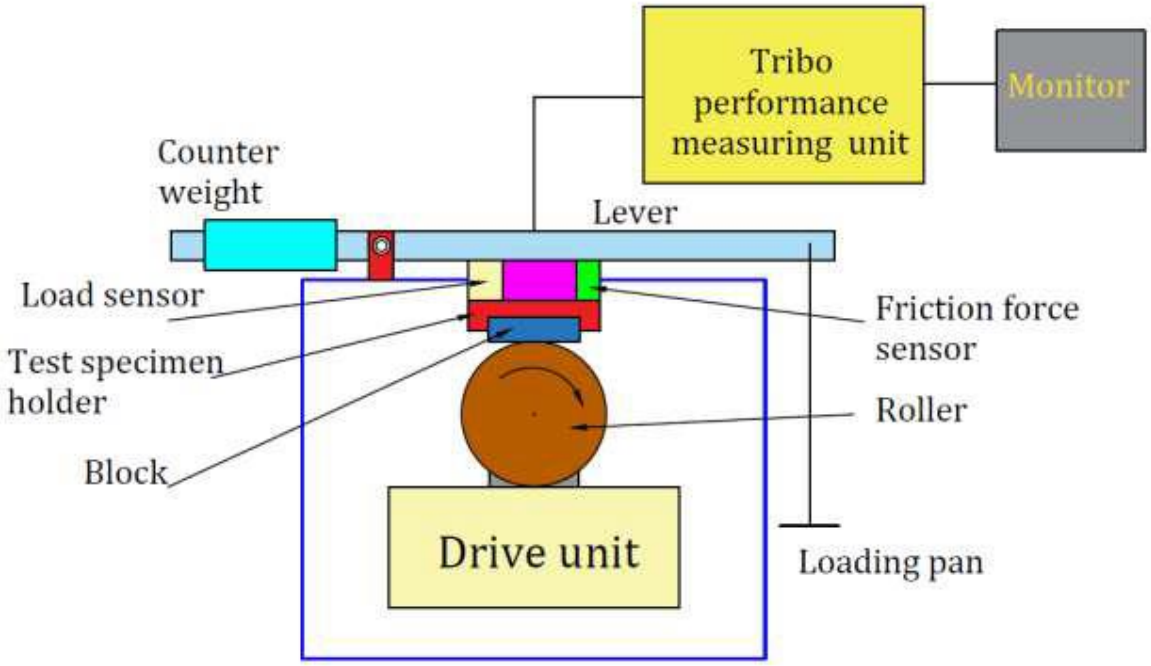

Figure 2 (a): Schematic representation of multi tribo tester

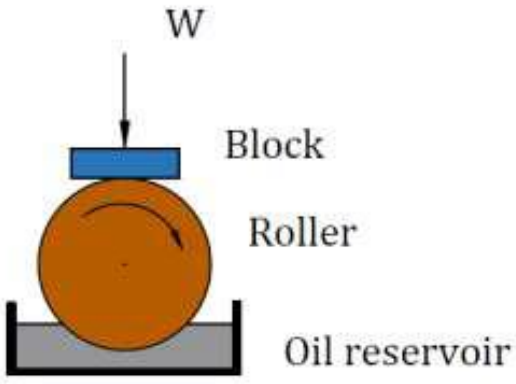

Figure 2(b): Contact geometry of test specimens

Tianjin Daxue Xuebao (Ziran Kexue yu Gongcheng Jishu Ban)/
Journal of Tianjin University Science and Technology
ISSN (Online):0493-2137
E-Publication: Online Open Access
Vol: 55 Issue: 10:2022
DOI: 10.5281/zenodo.19248091

4.2. Test parameters

4.2.1 Test specimen material

Figure 3 shows the optical microscope image of test specimen surface structures employed for the experimental investigations. The experiments are performed on test specimen made up of AISI chrome alloy standard steel No. E- 52100.Chemical composition of test specimen is 96.5 - 97.32 % Fe, 1.30 - 1.60% Cr; 0.980 - 1.10% C; 0.250 - 0.450% Mn; 0.150 - 0.300% Si; S≤ 0.0250%; P≤ 0.0250%. and 62 HRC. It is used in bearings in rotating machinery.

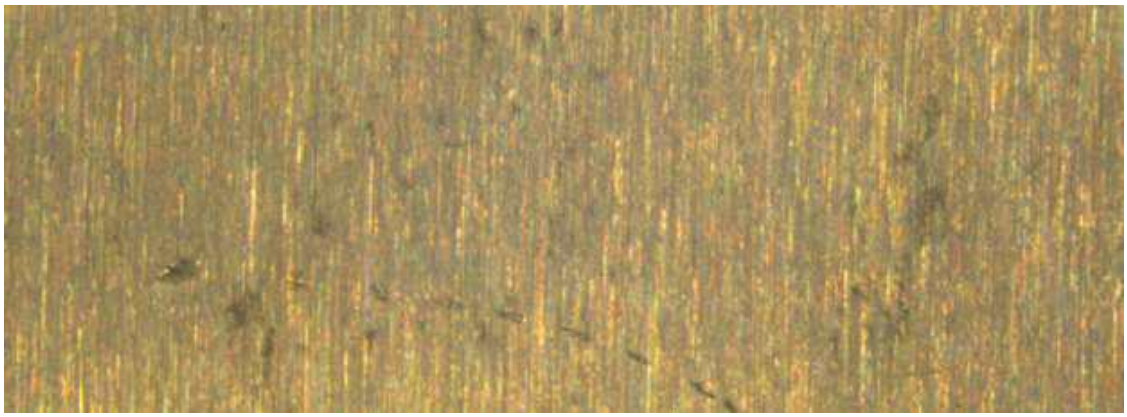

Figure 3: Microscope pictures of test specimen surfaces before test run

4.2.2 Lubricant

In the present experimental investigation, the selected lubricants are Servo Gear HP 140 and SAE 75W80. Servo Gear HP 140 oil and SAE 75W90 are recommended for light and heavy vehicle (passenger car, bus and highway truck) hypoid, worm gear axles, spiral bevel and also manual transmission for which an extreme pressure gear lubricant is required.

5. RESULTS

By using the mathematical model and experimental study, the effect of Servo Gear HP 140 and Gear oil 75W80 lubricant starvation upon pressure spike distribution and fluid film profile in starved EHL line contacts has been investigated. Present study of commercial oils starvation was performed simply by shifting position of the inlet meniscus from X_{in} = −6 to X_{in} = −1.25 closer to the Hertizian contact. The inlet contact zone is to the left and the outlet contact zone is to the right. Using an EHL model for line contacts under starvation lubricant conditions, it has been indicated that the film forming behavior is different from conventional EHL contacts

5.1 Pressure distributions and film profiles under Starvation of lubricant regime

The variation in percentage of starvation is shown in figure 4, for different loads and speeds respectively. It is observed from figure 4 that percentage of starvation varies with

Tianjin Daxue Xuebao (Ziran Kexue yu Gongcheng Jishu Ban)/
Journal of Tianjin University Science and Technology
ISSN (Online):0493-2137
E-Publication: Online Open Access
Vol: 55 Issue: 10:2022
DOI: 10.5281/zenodo.19248091

the position of inlet meniscus. As the position of inlet meniscus shifts towards contact zone an increase in percentage of starvation is observed with increase in speed. Figures 5 and 6 compares the pressure and fluid film profiles for lubricant oils servo gear HP 140 and gear oil 75W80 at different inlet distance i.e., X_{in} = −4 , X_{in} = −2 and X_{in} = −1.25 U = 3 × 10^{-11}; U = 5 × 10^{-11}.From 5 (ab), it can be seen that the reduction in the pressure spike is higher for the case SAE gear oil 75W80 with X_{in} = −1.25; U = 3 × 10^{-11}, the corresponding fluid film is much thinner than that of X_{in} = −4 and X_{in} = −2 under starvation lubricant condition in EHL contact. Further, from 6 (a-b), it can be noticed that H_{min} decreases substantially with shifting value of inlet distance (X_{in}) towards Hertizian contact zone. Obviously, this decrease in fluid film thickness and pressure spike are attributed to lower inlet zone viscosity which decreases with inlet region pressure as well as pressure-viscosity coefficient [22]. It has been seen that the H_{cent} also decreases by nearly the same factor as H_{min}. Thin fluid film thickness is attributes more starvation effect at higher speed. In order to investigate the influence of operating conditions on the SAE gear oil 75W80 and servo gear HP 140 behaviour under starved lubricant condition, Figure 7 presented the variation of pressure spike and fluid film profiles with inlet meniscus X_{in} = −4 , X_{in} = −2 and X_{in} = −1.25 . It is quite apparent that gear oil 75W80 behavior causes substantial reduction in the film thickness and pressure spike. It can be observed that pressure spike and fluid film thickness decreases with increasing inlet meniscus X_{in} = −4, X_{in} = −2 and X_{in} = −1.25 moves towards Hertizian contact. As indicated in the figures, the pressure spike and fluid film thickness decrease in servo gear HP 140 is much lower than that for SAE gear oil 75W80. Starvation causes lower pressure with a consequent decrease in viscosity and hence, pressure spike and fluid film thickness. The aforesaid decrease in film thickness and pressure spike is caused by lower contact zone viscositydue to localized pressure peaks.

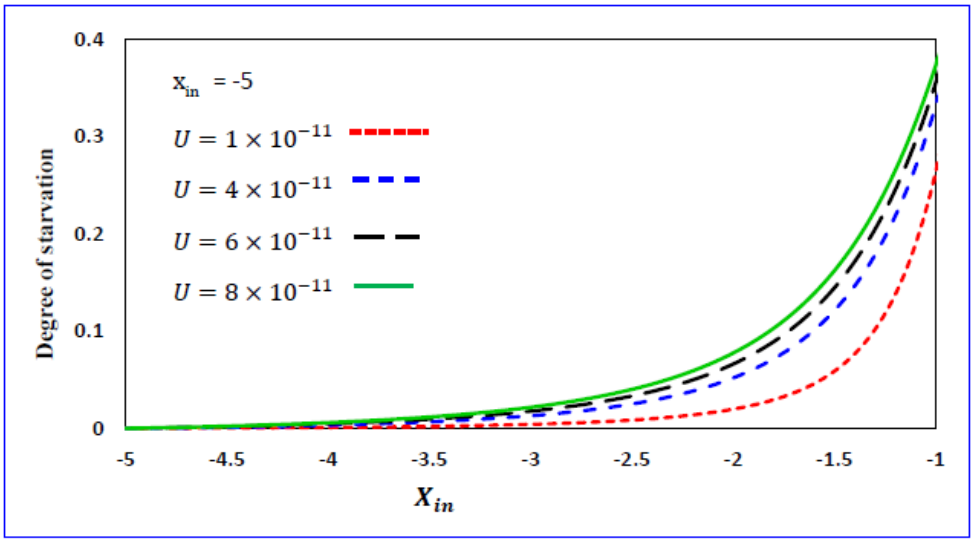

Figure 4: Variation of the degree of starvation with the position of the inlet meniscus for different

Tianjin Daxue Xuebao (Ziran Kexue yu Gongcheng Jishu Ban)/
Journal of Tianjin University Science and Technology
ISSN (Online):0493-2137
E-Publication: Online Open Access
Vol: 55 Issue: 10:2022
DOI: 10.5281/zenodo.19248091

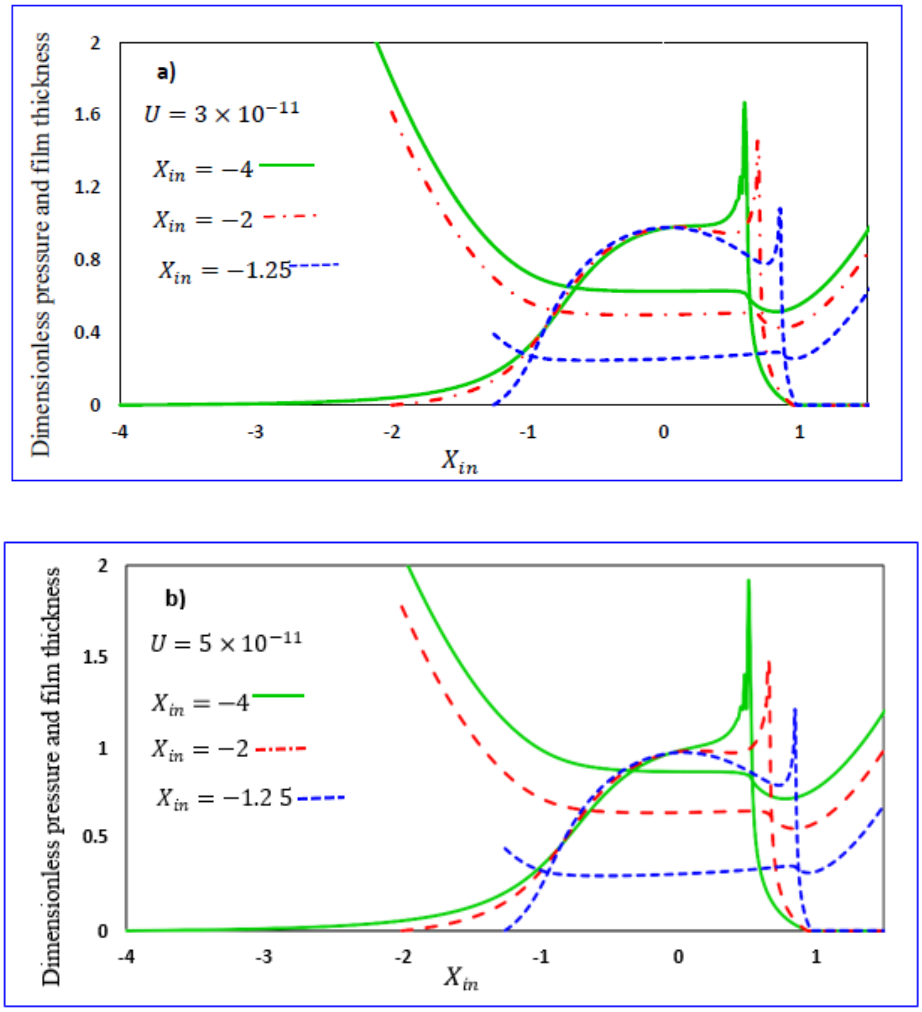

Figure 5: Comparison of film profiles and pressure distributions at different positions of inlet contact for Gear oil 75W80

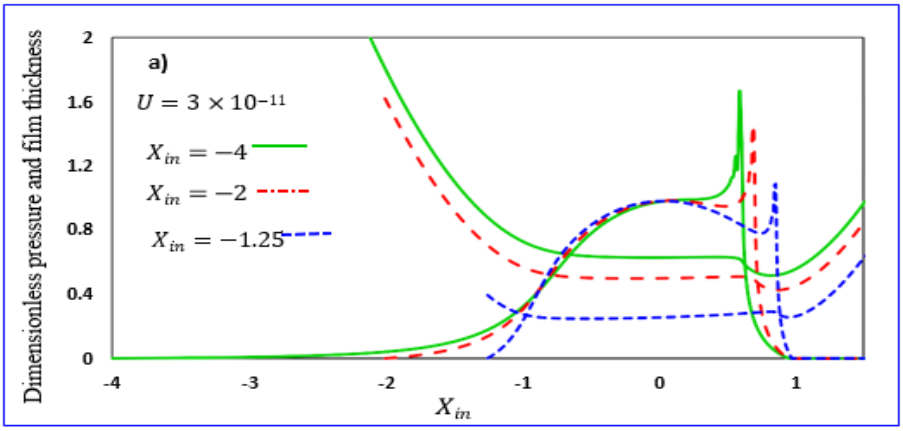

Tianjin Daxue Xuebao (Ziran Kexue yu Gongcheng Jishu Ban)/
Journal of Tianjin University Science and Technology
ISSN (Online):0493-2137
E-Publication: Online Open Access
Vol: 55 Issue: 10:2022
DOI: 10.5281/zenodo.19248091

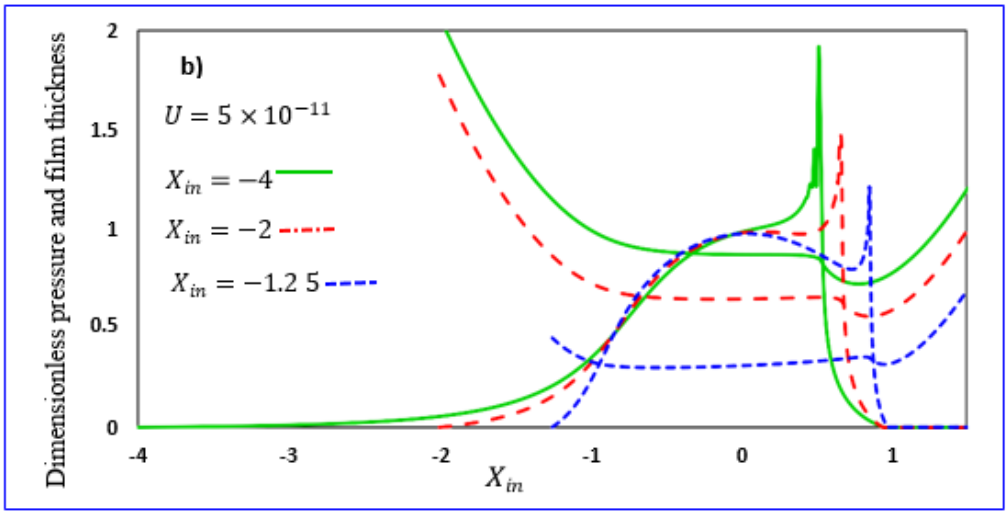

Figure 6: Comparison of film profiles and pressure distributions at different positions of inlet contact for Servo Gear HP 14

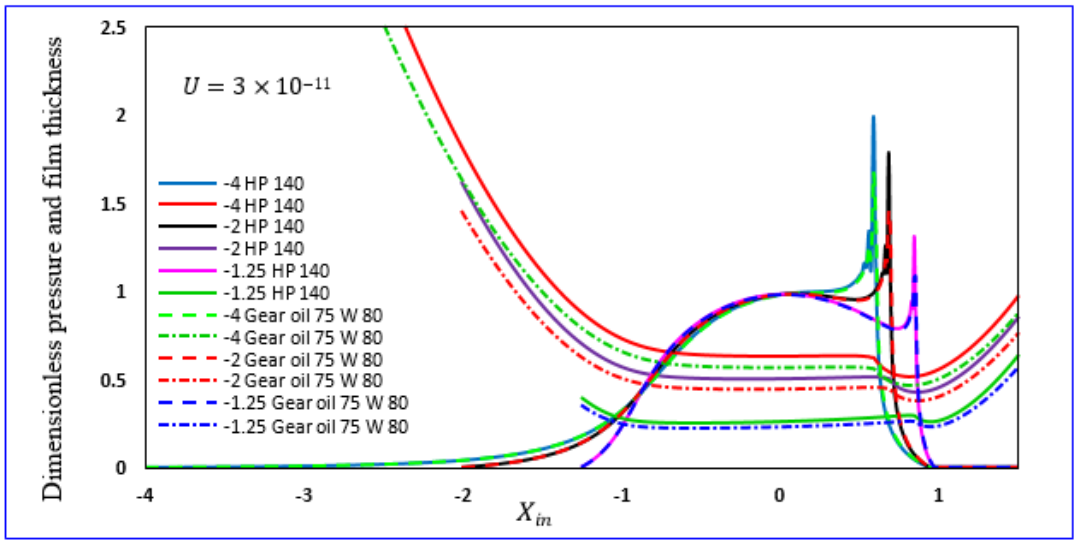

Figure 7: Comparison of fluid film profiles and pressure distributions at different positions of inlet contact

5.2 Contact friction

Figure 8 illustrates the variation of contact friction and 3D surface plots also present the increment in the contact friction of SAE75 W80 in comparison with servo gear oil HP140. The results showed an increase in contact friction with increasing values of velocity in the starvation of lubrication regime. It can be clearly seen that that the Servo gear HP 140 not only yields a much lower contact friction throughout but also a smaller variation in its value. Also, it forms equally thick EHL film as Gear oil 75W80 which yields much higher contact

Tianjin Daxue Xuebao (Ziran Kexue yu Gongcheng Jishu Ban)/
Journal of Tianjin University Science and Technology
ISSN (Online):0493-2137
E-Publication: Online Open Access
Vol: 55 Issue: 10:2022
DOI: 10.5281/zenodo.19248091

friction with maximum fluctuation in its value. Therefore, Servo gear HP 140 is a better choice in case lower power loss along with smooth and vibration-free operation is the primary selection criterion. On the other hand, Servo gear HP 140, yields the same initial value of contact friction as Gear oil 75W80 with a much thicker EHL film. Therefore, Servo gear HP 140 may be preferred over Gear oil 75W80, if larger film thickness is of prime importance. From figure 9(a-c). Intermittent peaks and contact friction rise has been observed for the case of SAE75 W80. This can be attributed that the thin fluid film thickness present in the non-conformal contact element and the X_{in} meniscus position moves towards Hertizian contact zone. Servo gear oil HP140 yields thicker fluid film thickness and the contact friction is lower than the SAE75 W80. Optical micro scope images at the end of experimentation reveal mixed to boundary lubrication condition for all worn out test specimen surface structures (optical images10(WTS1-WTS5) and 11(WTS1-WTS5) of both oil). Shallow scratches and wear tracks are seen on the substrate of worn out test specimen surface structures. Shallow scratches and wear tracks produced thinner fluid films under starved lubrication condition and tends to produce higher contact friction. From figures 8-9(a-c), comparative study of servo gear oil HP140 and SAE75 W80, SAE75 W80 is low viscosity oils and yield EHL films much thinner than the servo gear oil HP140. It can be seen that H_{min} decreases substantially with shifting X_{in} meniscus distance closer to Hertizian contact zone and this decrease is highly sensitive to pressure-viscosity coefficient. Obviously, this decrease in film thickness is attributed to lower inlet region viscosity which decreases with inlet zone pressure as well as pressure-viscosity coefficient. It has been noticed that the H_{cent} also decreases by nearly the same factor as H_{min} [5].

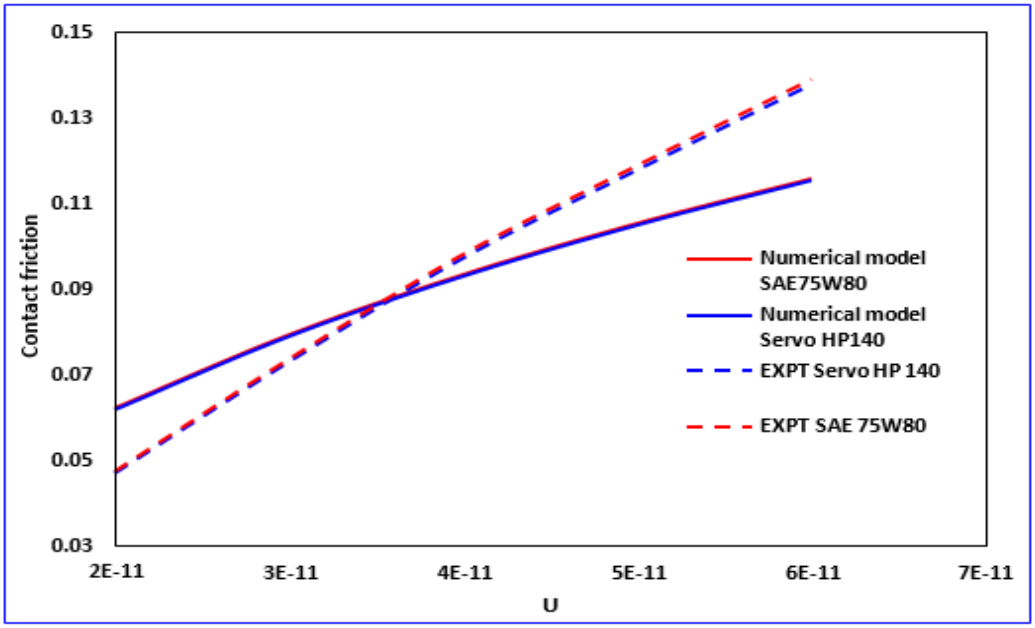

Figure 8: Comparison of contact friction for lubricant oil under starved lubrication condition

Tianjin Daxue Xuebao (Ziran Kexue yu Gongcheng Jishu Ban)/
Journal of Tianjin University Science and Technology
ISSN (Online):0493-2137
E-Publication: Online Open Access
Vol: 55 Issue: 10:2022
DOI: 10.5281/zenodo.19248091

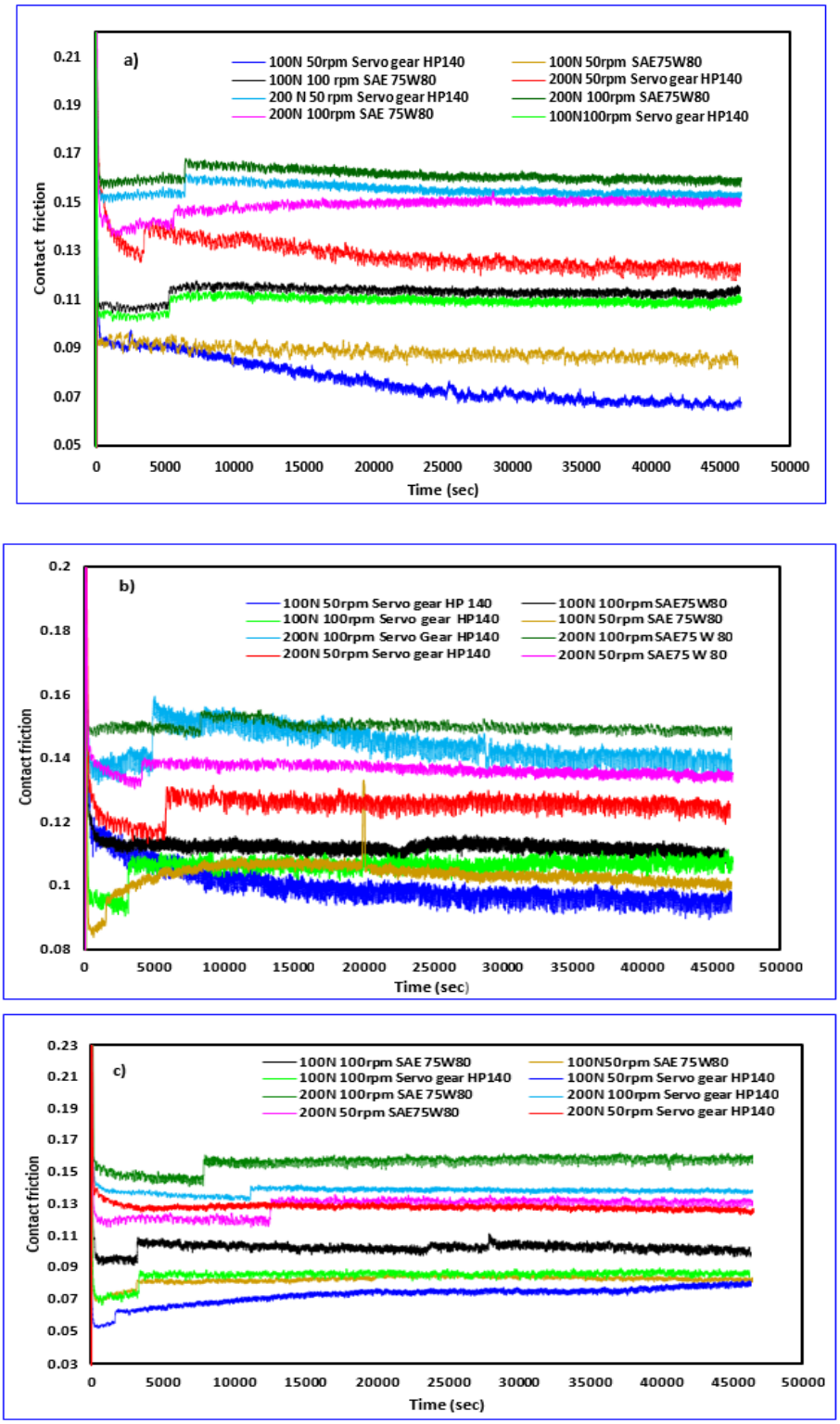

Figure 9: Variation of contact friction for different test sample

Tianjin Daxue Xuebao (Ziran Kexue yu Gongcheng Jishu Ban)/
Journal of Tianjin University Science and Technology
ISSN (Online):0493-2137
E-Publication: Online Open Access
Vol: 55 Issue: 10:2022
DOI: 10.5281/zenodo.19248091

5.3 Surface morphology

Figures 10 (WTS1-WTS5) and 11(WTS1-WTS5)- shows optical microscope images for worn out test specimen(WTS) under starved lubricant (HP140 and SAE 75W80) condition. The position of inlet meniscus moves closer to Hertizian contact from X_{in} = −4; X_{in} = −2 and X_{in} = −1.25. The worn out test specimen surfaces were subjected to elucidate the dominant mechanisms of material removal occurring under starved lubricant oil (HP140 and SAE 75W80) conditions. Optical microscope images of worn out test specimen surfaces lubricated with HP140 under starved lubricant condition are taken after 1hr duration of experimentation. Figure10, reveals light scratches in the circumferential direction and material removal rate has been measured. Wear track width of WTS1, WTS2, WTS3, WTS4, WTS5 and WTS6 lubricated with SAE 75W80 is found in the order of 0.753mm, 0.77mm, 0.737mm, 0.781mm, 0.768mm and 0. 702mm. Later, Figure 11 shows worn surfaces lubricated with SAE 75 W80.Under lubricant starvation condition, similar trend has been noticed in the figure 11.Mark of scratches slightly visible and measured width of each WTS1,WTS2,WTS3, WTS4, WTS5 and WTS6 lubricated with servo gear HP140 are 0.437mm, 0.488mm, 0.471mm, 0.62mm, 0.615mm and 0.617mm.The effect of surfaces waviness on worn out test specimens cannot be disregarded as waviness can cause seizure of two geometrically constrained sliding /rolling surfaces. Owing to the waviness, wear particles may be generated by high local friction forces. These particles may then wedge in between two geometrically constrained sliding/rolling surface and cause seizure.

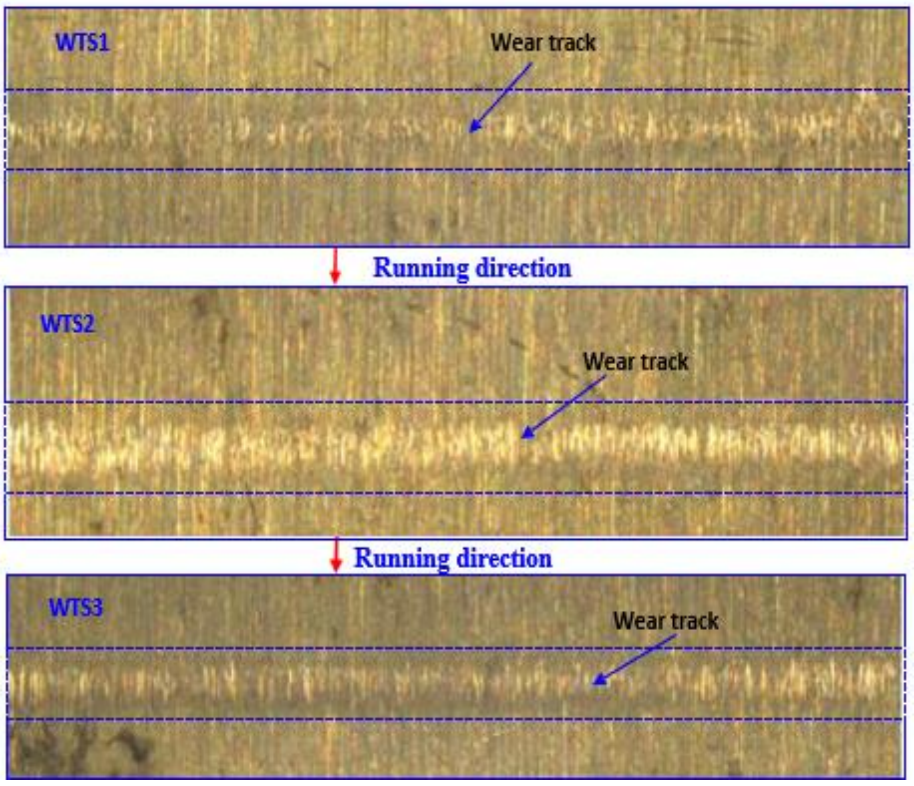

Tianjin Daxue Xuebao (Ziran Kexue yu Gongcheng Jishu Ban)/
Journal of Tianjin University Science and Technology
ISSN (Online):0493-2137
E-Publication: Online Open Access
Vol: 55 Issue: 10:2022
DOI: 10.5281/zenodo.19248091

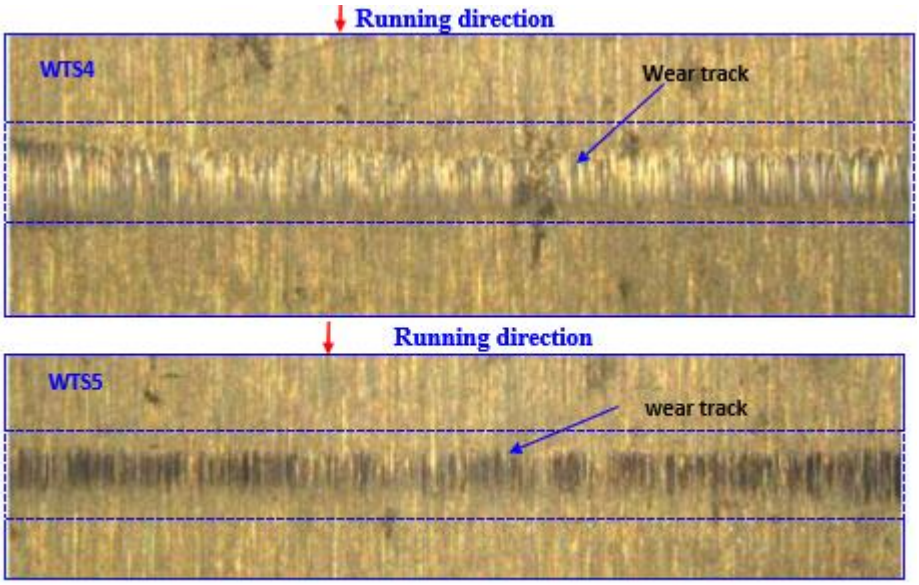

Figure 10: Optical micro scope images of worn out test specimens lubricated with Servo gear HP140

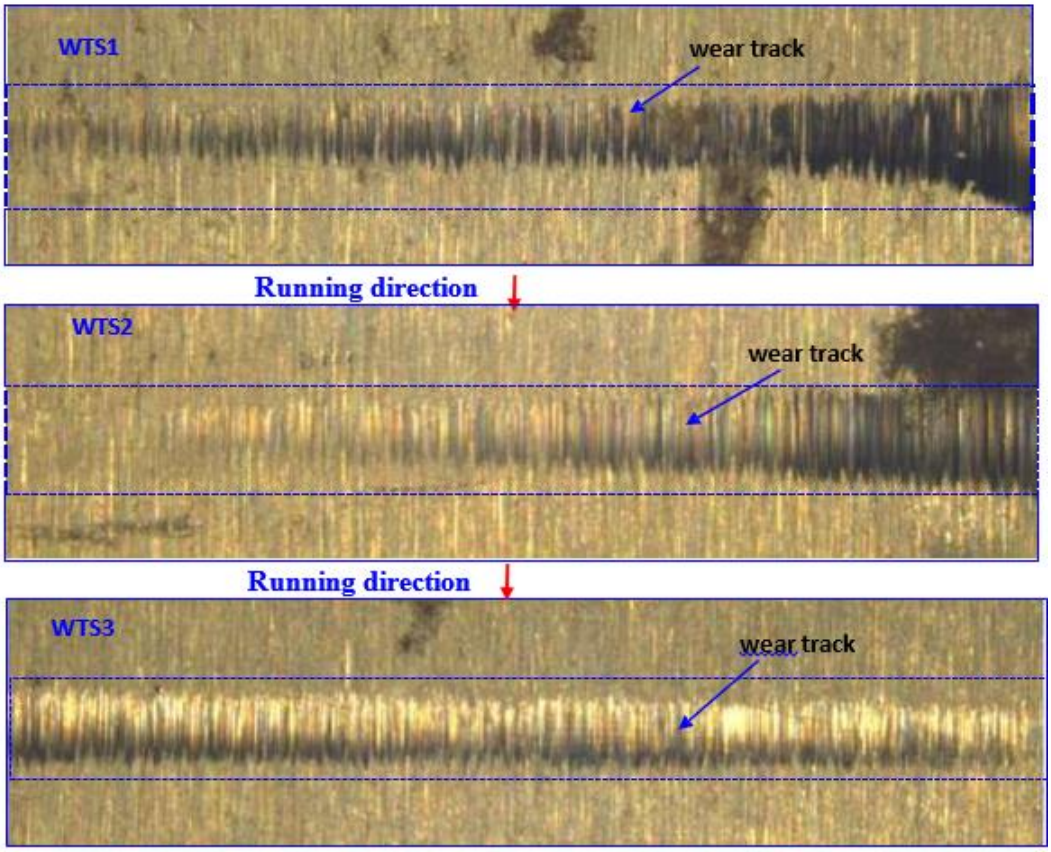

Tianjin Daxue Xuebao (Ziran Kexue yu Gongcheng Jishu Ban)/
Journal of Tianjin University Science and Technology
ISSN (Online):0493-2137
E-Publication: Online Open Access
Vol: 55 Issue: 10:2022
DOI: 10.5281/zenodo.19248091

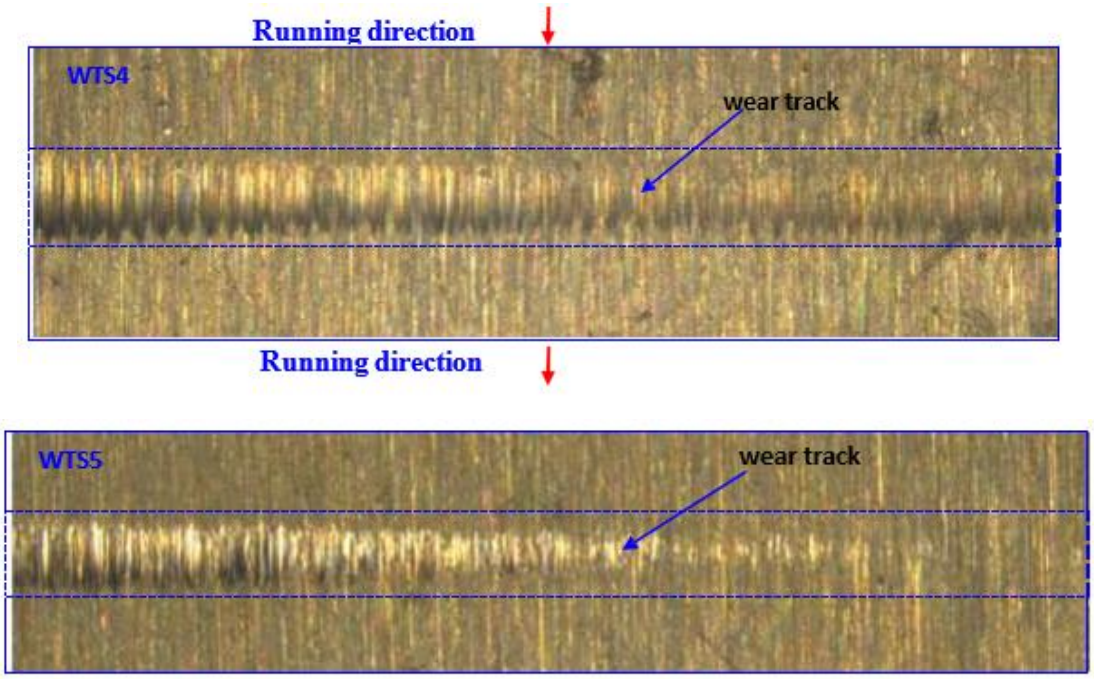

Figure 11: Optical micro scope images of worn out test specimens lubricated with SAE75W80

Optical profilometry (Taylor Hobson Talysurf) presents 3D and 2D profile of worn out test specimen (WTS)surfaces lubricated with servo gear oil HP140 and SAE 75W80 illustrated in the Figure 12 (WTS1-WTS4)-13(WTS1-WTS4).Obtained values of surface roughness parameter S_{sk} and $S_{ku}$are negative and positive. It implies that the lubricated worn out surface possess less load carrying capacity under starved lubricant condition. WTS1, WTS2, WTS3 and WTS4 lubricated with Servo gear oil HP140.Value of S_a is found to be 0.429 μm and 0.410 μm and S_{sk} is -0.685, -1.31 for WTS1 and WTS2. Similarly, WTS3 and WTS4 value of S_a for is 0.422 μm ,0.509 μm and S_{sk} is -0.277 and -1.18 for the case of WTS3 and WTS4.This indicates that the S_{sk} increase negatively and S_a positively ,which means formation of less peaks than valleys. Which is also verified that the increment in the value of S_v in comparison with S_p for all WTS surfaces. This specifies that the probable density of valleys is less compared to peaks during the starved lubrication regime [23]. Later, in the second stage of test run WTS lubricated with SAE 75W80 under starved lubricant condition.3D profile of WTS surfaces is presented in the figure 8b. Figure 8b shows the existence of valleys and peaks due to the S_{sk} and S_k . S_{sk} increase -0.228, -0.278, -0.32 and -0.405 and increment in the value of S_{ku} in the order of 2.74 μm,2.91 μm, 3.15 μm, 3.37 μm . S_{sk} and S_{ku} are negatively and positively increased, which means density of valleys is more than that of peaks. Thus, reduction in the fluid film is substantially with increasing value of X_{in} inlet meniscus distance closer to the Hertizian contact. From Figure 12(WTS1-WTS4)- 13(WTS1-WTS4),spiky asperities has been observed on the WTS surfaces through the 3D optical profilometry technique because of S_{sk} and S_{ku} values are >3. Gaussian distribution of asperities is

Tianjin Daxue Xuebao (Ziran Kexue yu Gongcheng Jishu Ban)/
Journal of Tianjin University Science and Technology
ISSN (Online):0493-2137
E-Publication: Online Open Access
Vol: 55 Issue: 10:2022
DOI: 10.5281/zenodo.19248091

seen on the worn surfaces due to the presence of S_q/S_a. In lubricated contact S_q plays vital role and it represents composite surface roughness, which decides λ ratio in the EHL regime. The minimum film thickness decreased due to the presence of S_q and S_z. Besides, a reduction in the value of minimum film thickness was observed, whereas, the contact friction was found to increase with an increase in S_z, S_a. S_z, S_a, S_v , S_{sk} , S_{ku} and S_q not only interacts with the hydrodynamics of the fluid film but it also leads to very high local contact pressures near the asperity tip regions where the fluid film is not thick enough to separate the contacting surfaces completely. This phenomenon is responsible for causing the collapse of the fluid film, which leads to either failure of the lubrication system or change of lubrication from full film to mixed EHL. Figure 12(WTS1-WTS5)-13(WTS1-WTS4) compares the 3D and 2D profiles for servo gear oil HP140 and SAE 75W80 under starved lubricant condition. Wear track is occurs, when the value of S_v is lower or higher than this rage 0.3 $\mu m \leq S_v \leq 2\mu m$, rolling wear occurs[24].It can be seen that the depth of valley/wear track is much lower for the case of servo gear oil HP140.

1)

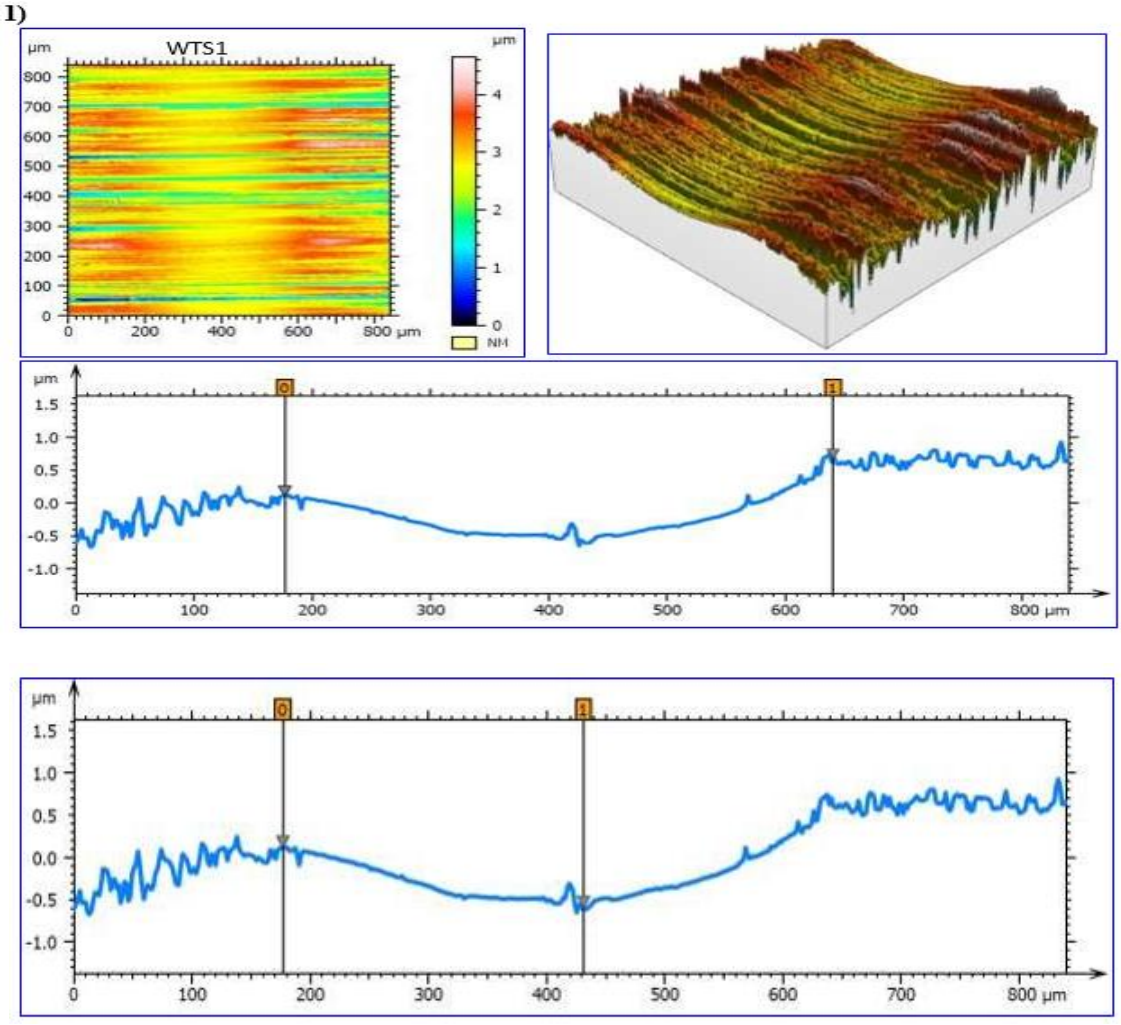

Tianjin Daxue Xuebao (Ziran Kexue yu Gongcheng Jishu Ban)/
Journal of Tianjin University Science and Technology
ISSN (Online):0493-2137
E-Publication: Online Open Access
Vol: 55 Issue: 10:2022
DOI: 10.5281/zenodo.19248091

2)

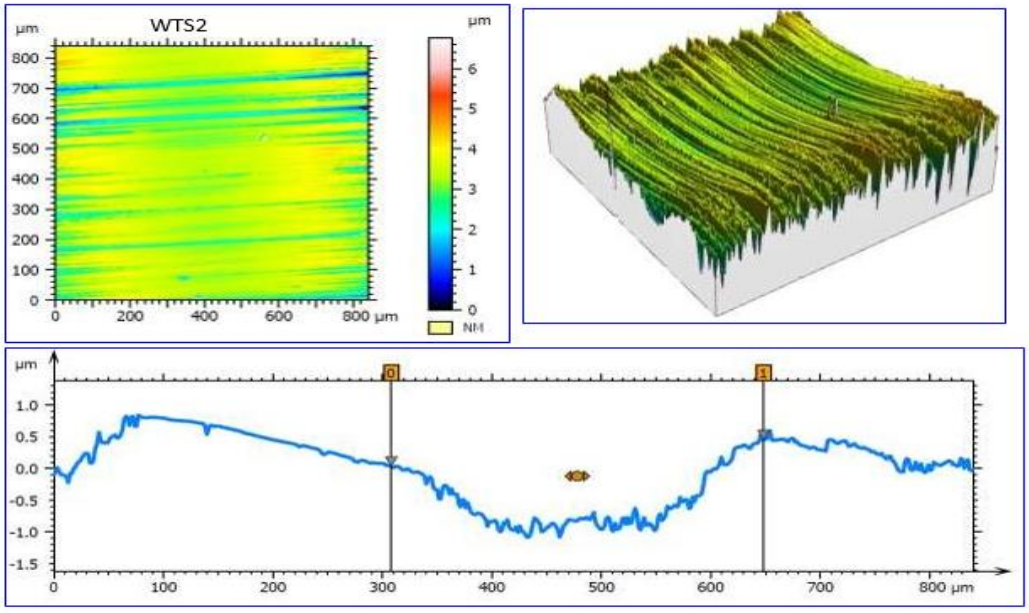

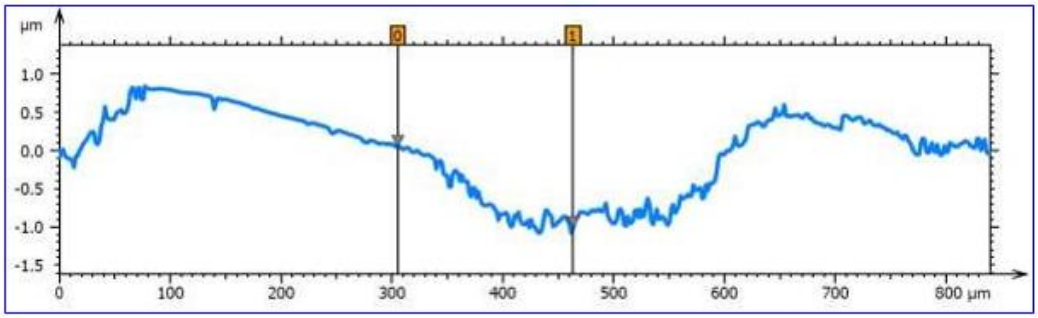

3)

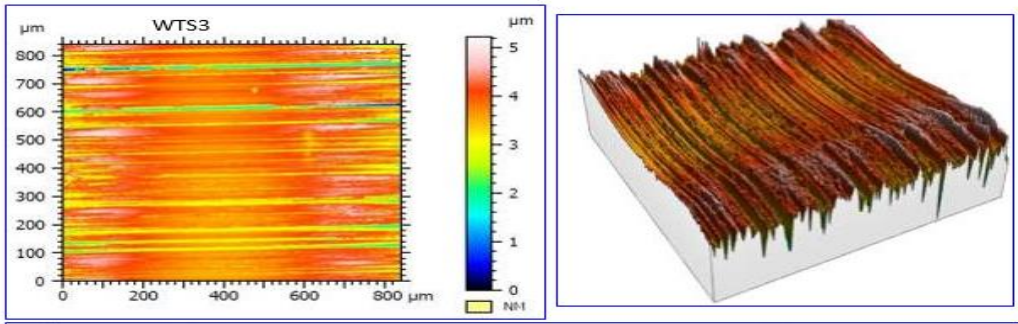

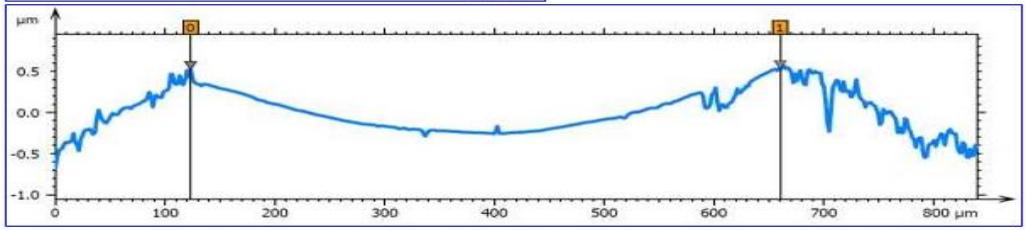

Tianjin Daxue Xuebao (Ziran Kexue yu Gongcheng Jishu Ban)/
Journal of Tianjin University Science and Technology
ISSN (Online):0493-2137
E-Publication: Online Open Access
Vol: 55 Issue: 10:2022
DOI: 10.5281/zenodo.19248091

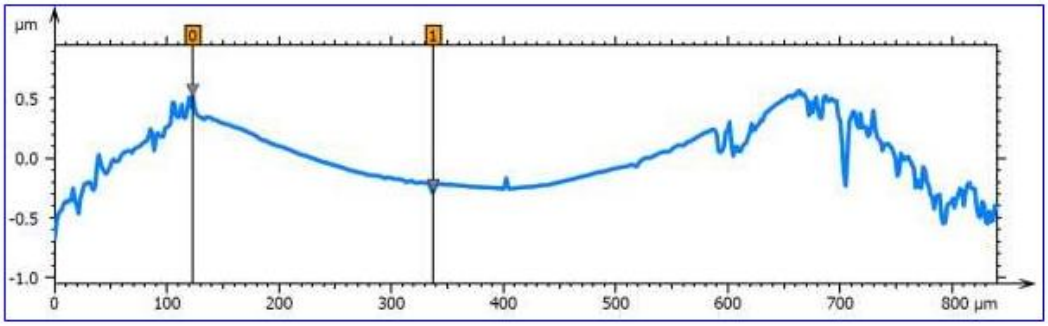

4)

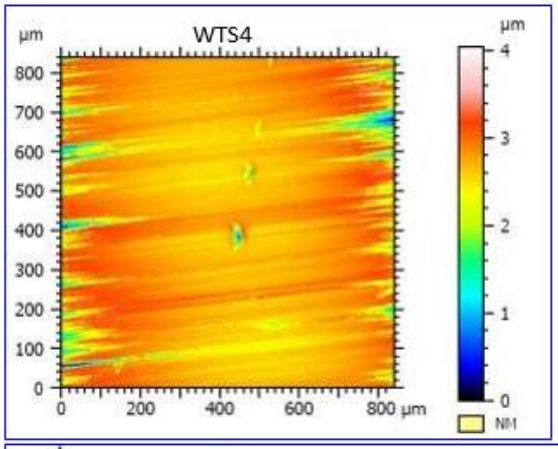

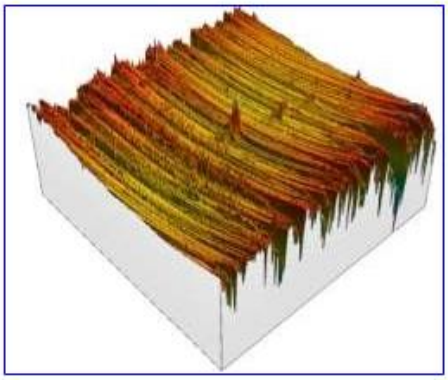

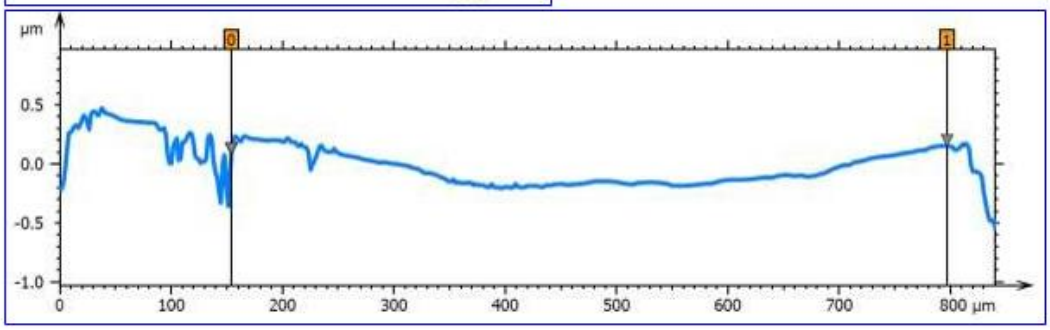

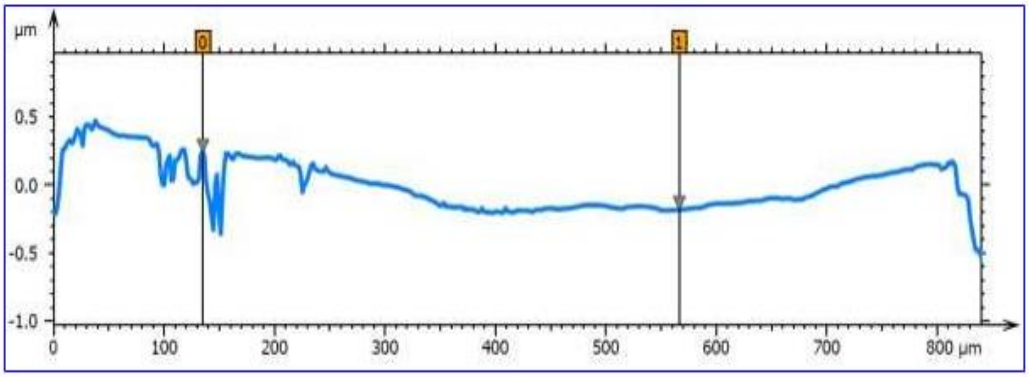

Tianjin Daxue Xuebao (Ziran Kexue yu Gongcheng Jishu Ban)/
Journal of Tianjin University Science and Technology
ISSN (Online):0493-2137
E-Publication: Online Open Access
Vol: 55 Issue: 10:2022
DOI: 10.5281/zenodo.19248091

5)

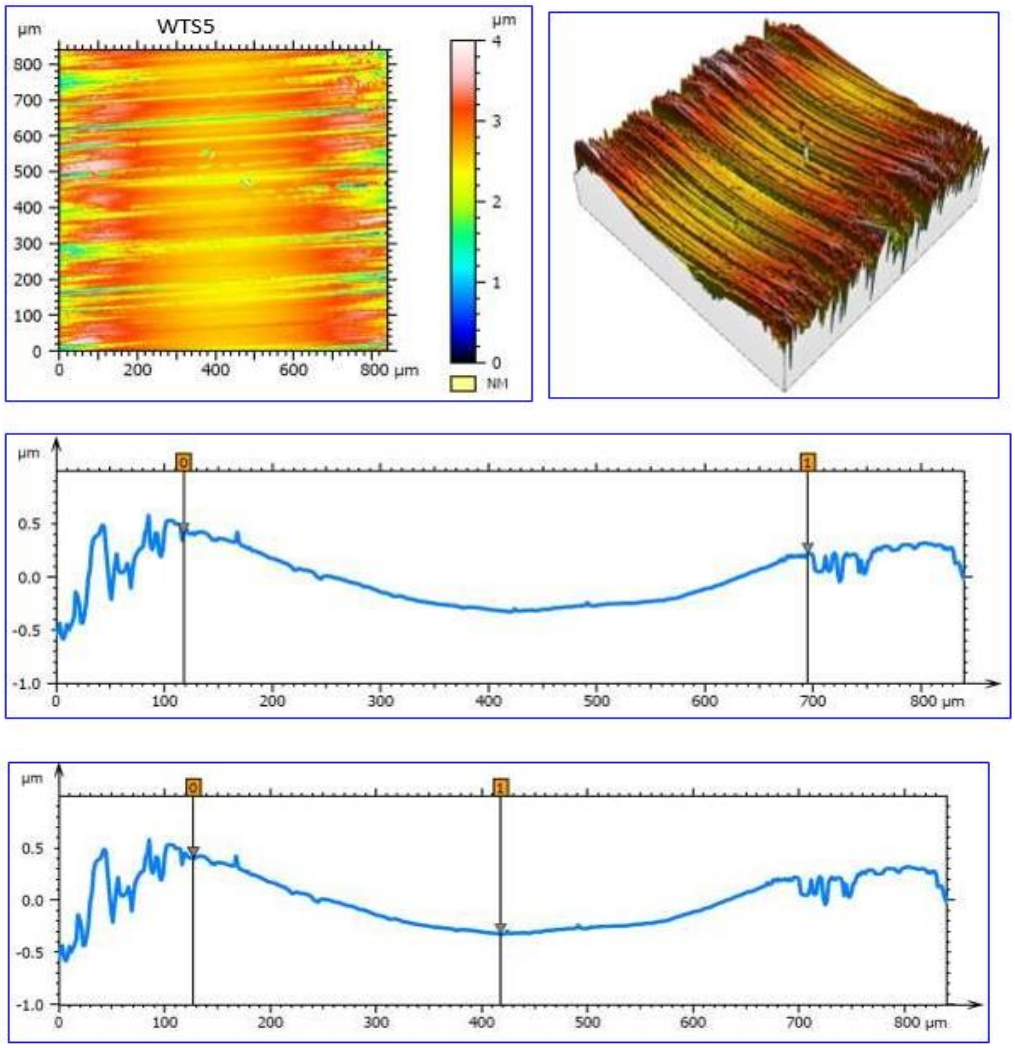

Figure 12: 3D and 2D profile of worn out test specimen lubricated with servo gear oil HP140

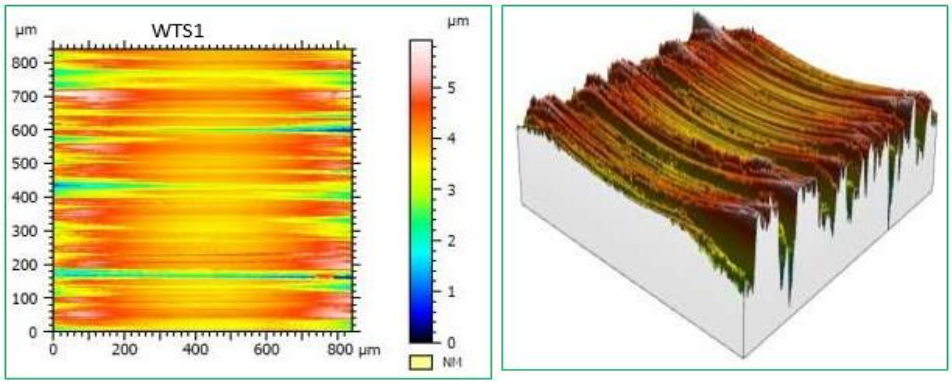

Tianjin Daxue Xuebao (Ziran Kexue yu Gongcheng Jishu Ban)/
Journal of Tianjin University Science and Technology
ISSN (Online):0493-2137
E-Publication: Online Open Access
Vol: 55 Issue: 10:2022
DOI: 10.5281/zenodo.19248091

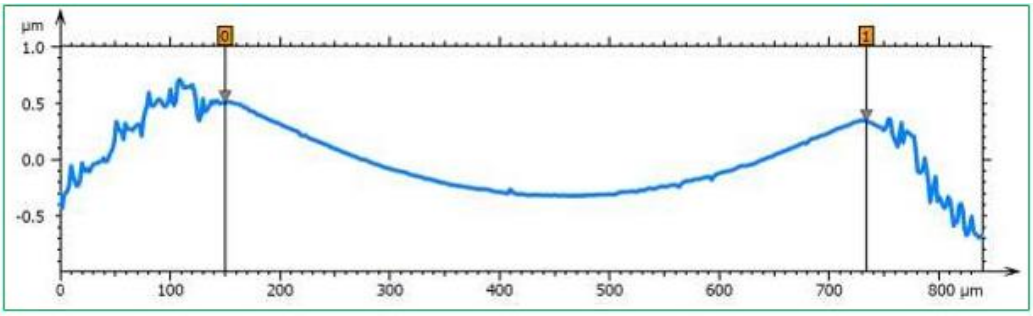

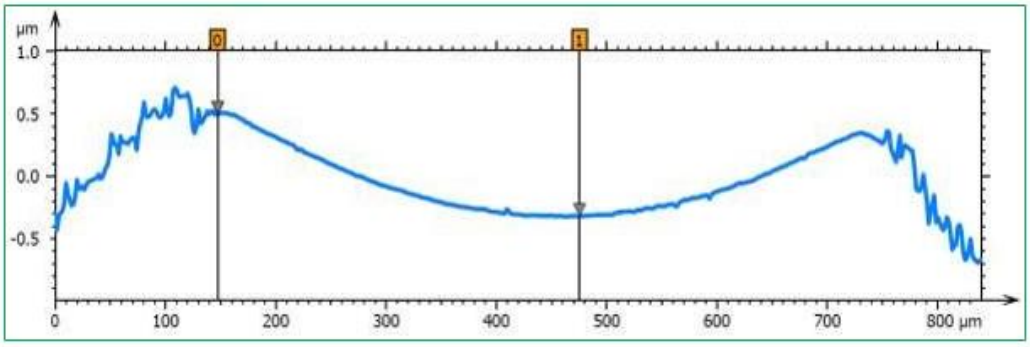

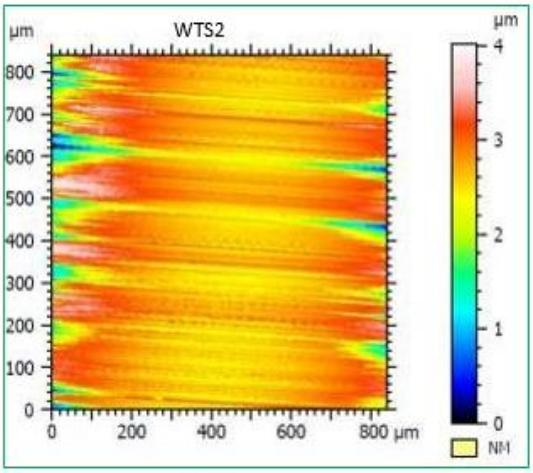

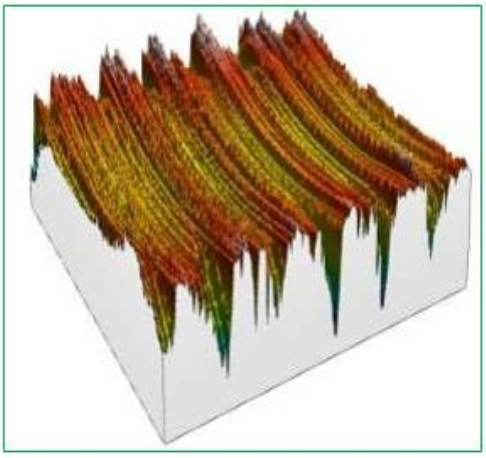

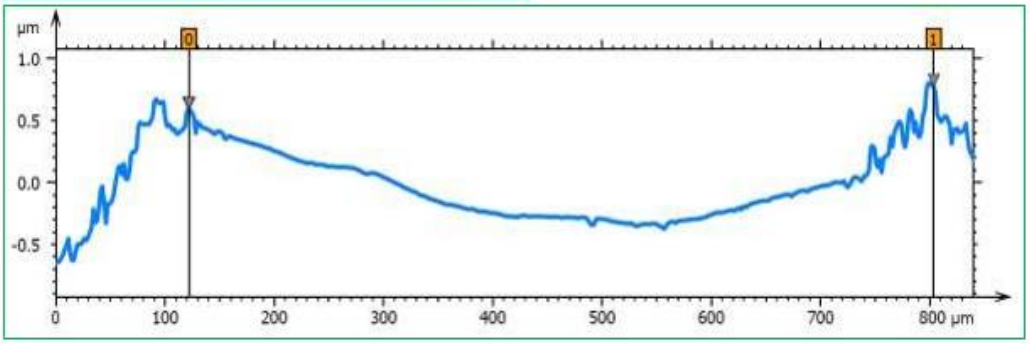

Tianjin Daxue Xuebao (Ziran Kexue yu Gongcheng Jishu Ban)/
Journal of Tianjin University Science and Technology
ISSN (Online):0493-2137
E-Publication: Online Open Access
Vol: 55 Issue: 10:2022
DOI: 10.5281/zenodo.19248091

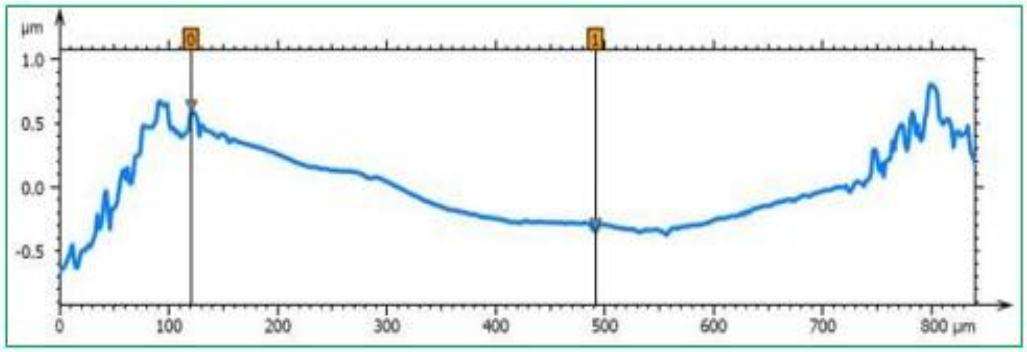

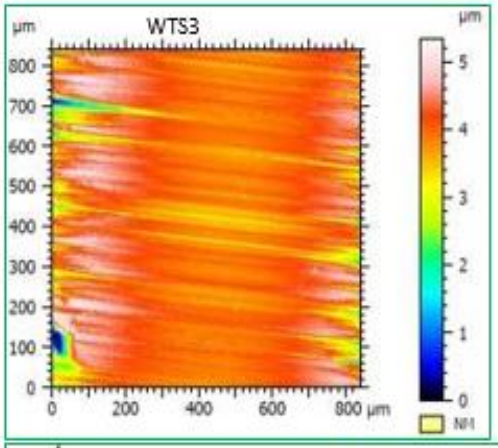

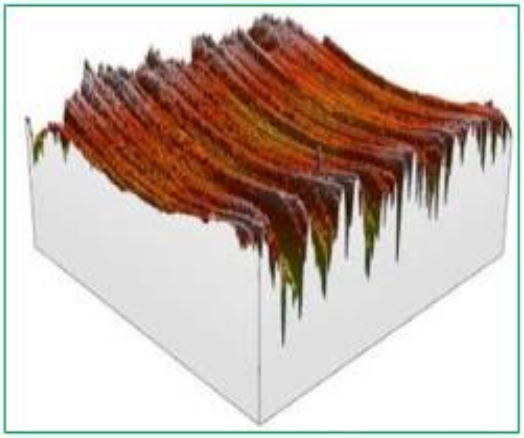

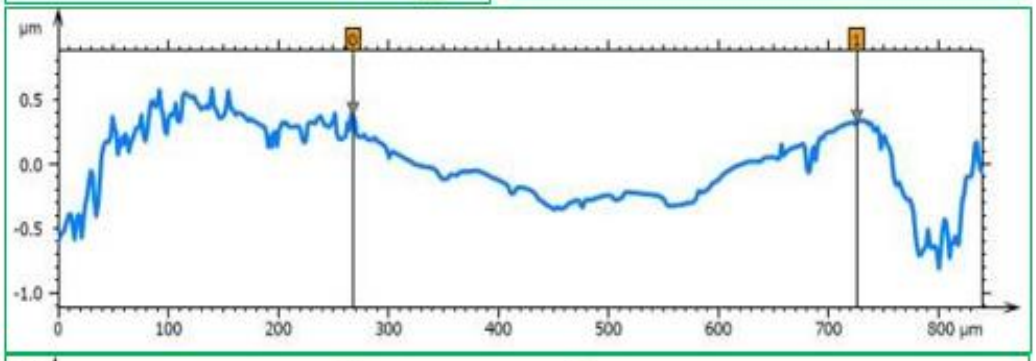

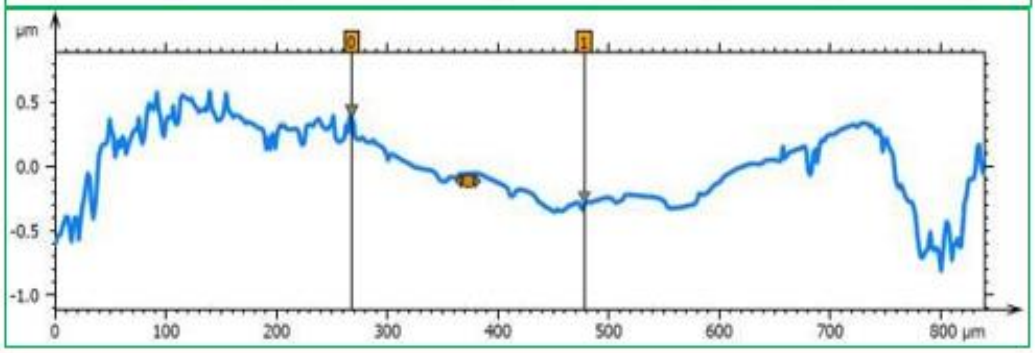

Tianjin Daxue Xuebao (Ziran Kexue yu Gongcheng Jishu Ban)/
Journal of Tianjin University Science and Technology
ISSN (Online):0493-2137
E-Publication: Online Open Access
Vol: 55 Issue: 10:2022
DOI: 10.5281/zenodo.19248091

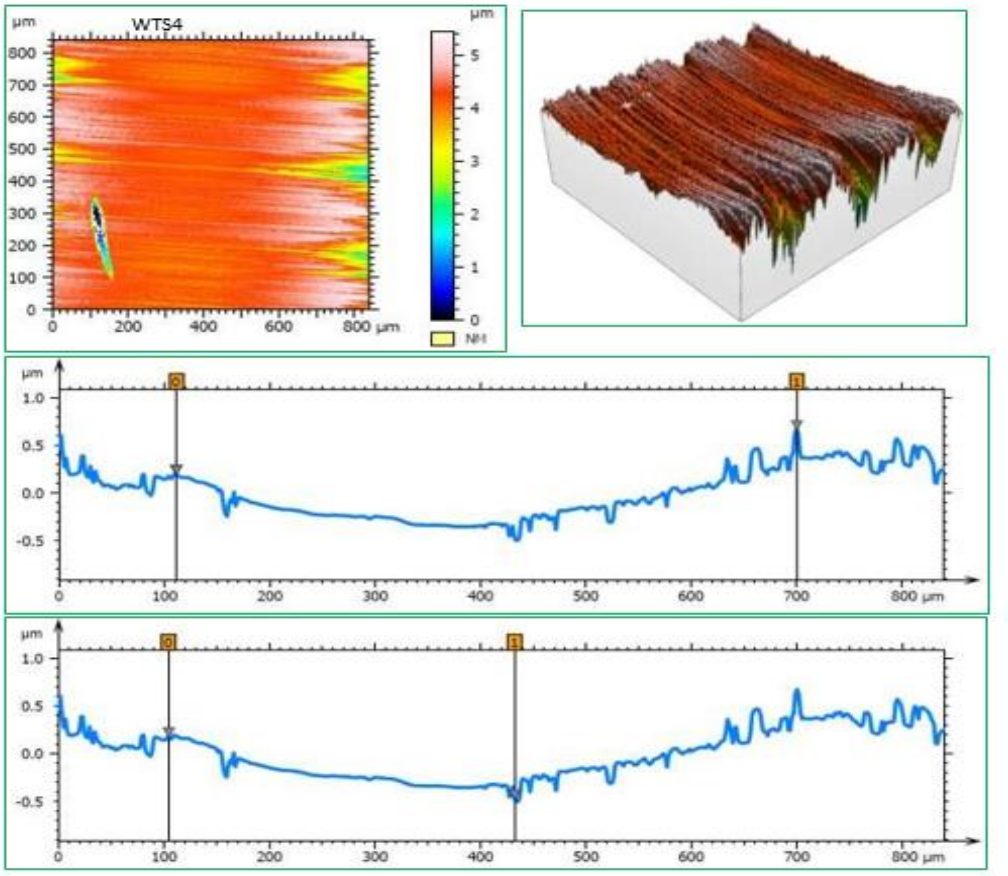

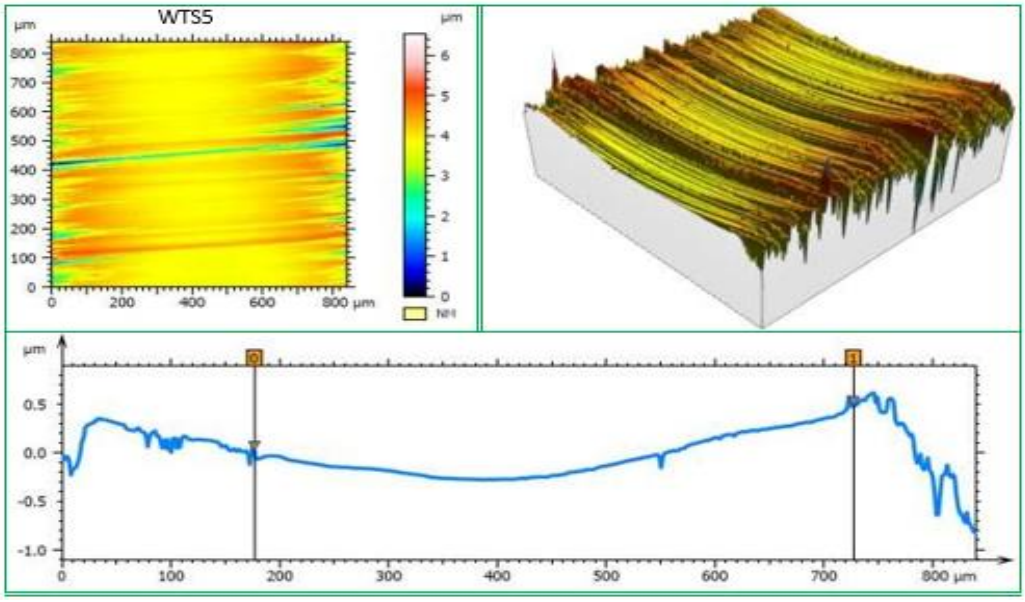

Tianjin Daxue Xuebao (Ziran Kexue yu Gongcheng Jishu Ban)/
Journal of Tianjin University Science and Technology
ISSN (Online):0493-2137
E-Publication: Online Open Access
Vol: 55 Issue: 10:2022
DOI: 10.5281/zenodo.19248091

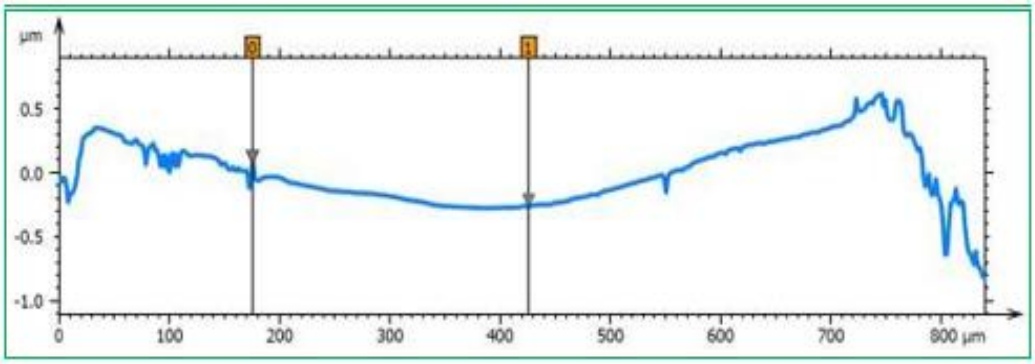

Figure13: 3D and 2D profile of worn out test specimen (WTS) lubricated with SAE 75W80

6. CONCLUSIONS

In this paper, effect of lubricant starvation on the Tribo-performance of EHD line contact have been studied through numerical simulation and experimental investigation on block-on roller tribo tester rig forms EHL line contact.

The deviations in the film thickness profile and pressure distribution are investigated. It is revealed that, normally, the influence of starvation on the film thickness is more pronounced. Consequently, the viscosity of the SAE75W80 oil was reduced higher than that of the HP 140.

The decrease of oil viscosity was attributed to the creation of comparatively thin oil films on sliding surfaces. This thin oil film has been associated with increased wear rates and friction. FE-SEM technique revealed, during the SAE 75W80 oil experiment, many micro-cracks occurred due to surface damage.

One of the reason for wear increased in test specimen lubricated with SAE75W80 oil has been surface damage. The development of a thin oxide layer increases the wear on the surface. Based on the features of the miscibility of SAE75W80, it is feasible that the quantity of miscible CO_2 may have increased with increasing pressure. Thus, the viscosity of the SAE75W80 oil decreased and the lubricant film was reduced on the sliding surface.

As a result, wear and friction increased as the actual metal contact area increased. The HP 140 is yield much lower contact friction, wear and slightly thicker EHL films than that of SAE 75W80 for a given set of operating conditions. Minimum variation in its value desirable for smooth and vibration-free operation in non-conformal EHL contacts.

The contacting inlet meniscus distance moves closer to Hertizian contacts under starved lubricant condition, leading to high contact friction and hence, high wear rate, it causes premature failure of the components. The application of present analysis is useful for lubricant selection in the rotating machinery.

Tianjin Daxue Xuebao (Ziran Kexue yu Gongcheng Jishu Ban)/
Journal of Tianjin University Science and Technology
ISSN (Online):0493-2137
E-Publication: Online Open Access
Vol: 55 Issue: 10:2022
DOI: 10.5281/zenodo.19248091

Nomenclature

$b=4R\sqrt{\frac{W}{2\pi}}$	: Half Hertzian contact width (m)	E'	: Effective elastic modulus (Pa)
H_0	: Offset film thickness	h	: Film thickness (m)
h_{min}	: Minimum fluid film thickness (m)	p	: Pressure (Pa)
$P_h=E'b/4R$	: Maximum Hertzian pressure (Pa)	R	: Equivalent radius of contact (m)
u_s	: Average rolling speed(m/s)	X_{in}	: Inlet contact
w	: External load per unit width	X_L	: Local co-ordinates
s	: Roeland's parameter		

Greek symbols

$\Omega=3U\pi^2/4W^2$	Speed factor	η_0	: Inlet viscosity of the lubricant (Pa-s)
$\bar{\eta}=\eta/\eta_0$	: Dimensionless viscosity	α	: Pressure-viscosity coefficient (Pa^{-1})
$\bar{\rho}=\rho/\rho_0$	: Dimensionless density	ρ	: Density (Kg/m^3)

Matrices

$[J]$	: Jacobian matrix	$\{p\}$	: Nodal pressure vector
$\{R\}$	: Hydrodynamic term	$[F]$	: Fluidity matrix

References

1) P. Cann, E. Ioannides, B. Jacobson, A. Lubrecht, The lambda ratio—a critical re-examination, Wear 175(1-2) (1994) 177-188.

2) C. Foord, Discussion:"Isothermal Elastohydrodynamic Lubrication of Point Contacts: Part IV—Starvation Results"(Hamrock, BJ, and Dowson, D., 1977, ASME J. Lubr. Technol., 99, pp. 15–23), Journal of Lubrication Technology 100(1) (1978) 142-142.

3) P. Goksem, R. Hargreaves, The effect of viscous shear heating on both film thickness and rolling traction in an EHL line contact—Part II: Starved conditions, Journal of Lubrication Technology 100(3) (1978) 353- 358.

4) I. Křupka, R. Poliščuk, M. Hartl, Behavior of thin viscous boundary films in lubricated contacts between micro-textured surfaces, Tribology International 42(4) (2009) 535-541.

5) U. Sudeep, R. Pandey, N. Tandon, Effects of surface texturing on friction and vibration behaviors of sliding lubricated concentrated point contacts under linear reciprocating motion, Tribology International 62 (2013) 198-207.

Tianjin Daxue Xuebao (Ziran Kexue yu Gongcheng Jishu Ban)/
Journal of Tianjin University Science and Technology
ISSN (Online):0493-2137
E-Publication: Online Open Access
Vol: 55 Issue: 10:2022
DOI: 10.5281/zenodo.19248091

6) L.D. Wedeven, D. Evans, A. Cameron, Optical analysis of ball bearing starvation, Journal of Lubrication Technology 93(3) (1971) 349-361.

7) Y. Chiu, An analysis and prediction of lubricant film starvation in rolling contact systems, ASLE transactions 17(1) (1974) 22-35.

8) J. Pemberton, A. Cameron, A mechanism of fluid replenishment in elastohydrodynamic contacts, Wear 37(1) (1976) 185-190.

9) E. Kingsbury, B. Schritz, J. Prahl, Parched elasto hydrodynamic lubrication film thickness measurement in an instrument ball bearing, Tribology transactions 33(1) (1990) 11-14.

10) E. Kingsbury, Cross flow in a starved EHD contact, Asle Transactions 16(4) (1973) 276-280.

11) P. Wolveridge, K. Baglin, J. Archard, The starved lubrication of cylinders in line contact, Proceedings of the Institution of Mechanical Engineers 185(1) (1970) 1159-1169.

12) H.G. Elrod, A cavitation algorithm, Journal of lubrication Technology 103(3) (1981) 350-354.

13) F. Chevalier, A. Lubrecht, P. Cann, F. Colin, G. Dalmaz, Film thickness in starved EHL point contacts, Journal of tribology 120(1) (1998) 126-133.

14) Y.H. Wijnant, Contact dynamics in the field of elastohydrodynamic lubrication, Department of Mechanical Engineering, University of Twente1998.

15) B. Damiens, C.H. Venner, P. Cann, A. Lubrecht, Starved lubrication of elliptical EHD contacts, Journal of tribology 126(1) (2004) 105-111.

16) N. Biboulet, F. Colin, A. Lubrecht, Friction in starved hydrodynamically lubricated line contacts, Tribology International 58 (2013) 1-6.

17) M. Müller, G.-P. Ostermeyer, F. Bubser, A contribution to the modeling of tribological processes under starved lubrication, Tribology International 64 (2013) 135-147.

18) D. Dowson, G. Higginson, Elasto-hydrodynamic Lubrication Pergamon Press, Oxford Google Scholar, 1966.

19) C. Roelands, J. Vlugter, H. Waterman, The viscosity-temperature-pressure relationship of lubricating oils and its correlation with chemical constitution, Journal of Basic Engineering 85(4) (1963) 601-607.

20) H. Lu, M. Berzins, C. Goodyer, P. Jimack, High-order discontinuous Galerkin method for elastohydrodynamic lubrication line contact problems, International Journal for Numerical Methods in Biomedical Engineering 21(11) (2005) 643-650.

21) C.E. Goodyer, M. Berzins, P.K. Jimack, L. Scales, A grid-enabled problem solving environment for parallel computational engineering design, Advances in Engineering Software 37(7) (2006) 439-449.

22) P. Kumar, M. Khonsari, Combined effects of shear thinning and viscous heating on EHL characteristics of rolling/sliding line contacts, Journal of Tribology 130(4) (2008) 041505.

23) U. Effner, M. Woydt, Importance of machining on tribology of lubricated slip-rolling contacts of Si3N4, SiC, Si□N4 TiN and ZrO2, Wear 216(2) (1998) 123-130.

24) R. Kumar, S. Seetharamu, M. Kamaraj, Quantitative evaluation of 3D surface roughness parameters during cavitation exposure of 16Cr–5Ni hydro turbine steel, Wear 320 (2014) 16-24.

25) https://www.knowyourparts.com/technical-resources/engine/types-of-engine-bearing-damage

26) http://evolution.skf.com/us/white-etching-cracks-a-consequence-not-a-root-cause-of-bearing-failure